

Unified framework for outage-constrained rate maximization in secure ISAC under various sensing metrics

Hancheng Zhu, Zongze Li, Yik-Chung Wu

Abstract—Integrated sensing and communication (ISAC) is poised to redefine the landscape of wireless networks by seamlessly combining data transmission and environmental sensing. However, ISAC systems remain susceptible to eavesdropping, especially under uncertainty in eavesdroppers' channel state information, which can lead to secrecy outages. On the other hand, diverse and complex sensing performance requirements further complicate resource optimization, often requiring custom solutions for each scenario. To this end, this paper introduces a unified optimization framework that holistically addresses both the worst-case user secrecy rate and the sum secrecy rate across multiple users. Besides putting the two commonly used objectives into a single but flexible objective function, the framework accurately controls secrecy outage probabilities while accommodating a broad spectrum of sensing constraints. To solve such a general problem, we integrate the sensing requirements into the objective function through an auxiliary variable. This enables efficient alternating optimization and the proposed approach is theoretically guaranteed to converge to at least a stationary point of the original problem. Extensive simulation results show that the proposed framework consistently achieves higher optimized secrecy rates under various sensing constraints compared to existing methods. These results underscore the proposed unified framework's superiority and versatility in secure ISAC systems.

Index Terms—Integrated sensing and communication (ISAC), secure outage probability (SOP), max-min problem, secrecy rate optimization, sensing performance constraint.

I. Introduction

In the development of 6G networks, emerging applications such as autonomous driving, smart cities and virtual reality require high-precision sensing as well as high-quality communications [1]. As sensing systems and wireless communications share many similarities, the traditional way of separately designing these two systems may not be efficient enough in the future [2]. To address this challenge, integrated sensing and communication (ISAC) grows to be a promising technology due to its potential of saving resources from both systems without sacrificing performance [3].

In designing ISAC systems, a key is on balancing the performance of communications and sensing. In general, we can optimize the communication quality under sensing

requirement constraints or vice versa. However, as in conventional communication only systems, due to the open nature of wireless channels, the transmitted information from ISAC systems could be easily exposed to eavesdroppers, making the system vulnerable to unauthorized access and data breaches [4]. Therefore, secure ISAC has received increasing attention recently [5], [6].

In particular, to mitigate the adverse effects of eavesdroppers in secure ISAC, the most commonly employed strategy is through beamforming design [7]–[9]. Although these results are promising, the assumption of perfect channel state information (CSI) of the eavesdroppers' channels is often overly optimistic and impractical in real-world scenarios. Consequently, most existing studies focus on addressing the physical layer security (PLS) problem in ISAC systems with estimated eavesdropper channels. For example, [10]–[12] primarily aim to optimize beamforming strategies to reduce the detection probability of one or multiple eavesdroppers, thereby enhancing the security and reliability of the communication system. As a step further, techniques leveraging artificial noise [13], [14] and non-orthogonal multiple access (NOMA) [15], [16] have been proposed to improve secrecy performance, particularly in environments characterized by jamming or scattering.

Recently, emerging elements such as unmanned aerial vehicles (UAVs) [17] and intelligent reflective surfaces (IRS) [18], [19] have also been integrated into secure ISAC systems to counteract threats posed by multiple eavesdroppers. In these works, the eavesdropper channels are modeled with bounded errors [10]–[13], [15]–[19], or Gaussian error distributions [12], [14] around the true channels. For the bounded error case, [11] considers the average channel uncertainties through their sample mean. Moreover, robust system designs that account for the worst eavesdroppers' channel uncertainties are considered and solved either through linear matrix inequalities (LMIs) [10], [12], S-procedure [13], [15], [16], [18], [19] or quadratic reformulation [17]. When Gaussian errors are assumed, conservative methods such as Bernstein-type inequalities (BTI) [12], [14] are employed to ensure security constraints are satisfied. Although these estimated CSI assumptions are more realistic than the idealized perfect CSI, obtaining even the estimated channels of passive and covert eavesdroppers remains infeasible in many practical situations [20]. This challenge has been recognized in

Hancheng Zhu and Yik-Chung Wu are with the Department of Electrical and Electronic Engineering, The University of Hong Kong, Hong Kong (email: u3006551@hku.hk, ycwu@eee.hku.hk). Corresponding author: Zongze Li, Yik-Chung Wu.

Zongze Li is with the Peng Cheng Laboratory, Shenzhen 518038, China (e-mail: lizz@pcl.ac.cn).

PLS in other wireless systems [21]–[24], yet corresponding research in the context of secure ISAC systems remains limited.

On the other hand, in a multi-user setting, balancing performance among users is a critical challenge. Common objectives include worst-user rate maximization [7], [25]–[28] and weighted sum rate maximization [8], [29]–[31]. For example, [25], [29] leverage the mobility of UAVs to mitigate eavesdroppers’ risk via strategically planning UAV trajectories and beamforming at the base station (BS), thereby enhancing user transmission rates. Additionally, [28] employs a two-stage transmission protocol: initial environmental sensing followed by data transmission, to reduce the impact of eavesdroppers. Although both worst-user rate maximization and weighted sum rate maximization aim to optimize data transmission, existing studies typically treat these as independent problems. Notably, worst-user rate maximization is generally considered to be more challenging than sum rate maximization. This complexity arises from the discrete nature of selection variables in worst-user rate maximization problems. Current methods address this by employing deep reinforcement learning [27], or replacing the discrete selection with auxiliary variables [7], [25], [26], [28] and then convert it into a maximization framework. In contrast, sum rate maximization does not have such discrete handling steps, resulting in markedly different algorithmic approaches.

Apart from the differences in the objective function, sensing constraints in ISAC systems can also be markedly distinct. For instance, to ensure the desired performance of the sensing beampattern in radar-based ISAC systems under uncertain target location, [32]–[34] employ beampattern matching as a sensing metric. On the other hand, the signal-to-interference-plus-noise ratio (SINR) has been predominantly used as a measure of sensing signal quality and target tracking performance in various scenarios, including multiple-target single-user [35], single-target multi-user [36], and multiple-target multi-user systems [37], as well as cooperative ISAC networks [38] and two-cell interfering ISAC networks [39]. Due to the significant mathematical disparities among these sensing constraints, existing ways to manage these sensing requirements also vary substantially, ranging from successive convex approximation (SCA) [32], [34], [39], semidefinite relaxation (SDR) [33], [36], [38] to Taylor expansion [35].

The diversity in the objective functions and sensing constraints results in numerous combinations of different scenarios. Each of them typically requires separate investigation in the current practice. Not only does this demand considerable efforts, but the variety of ideas and techniques used across different studies also makes direct comparison between scenarios challenging. This paper aims to develop a unified optimization framework for these different secure ISAC scenarios. Such a framework not only enhances the adaptability of ISAC solutions across diverse sensing scenarios, but also enables fair and straightforward comparisons among different scenarios with minimal additional effort.

More specifically, to combine the worst case rate maximization and weighted sum rate maximization into a unified formulation, this paper for the first time proposes a general max-min problem which reduces to worst case rate maximization if the constraint of the inner minimization is a simplex. On the other hand, if the constraint of the inner minimization variables is a singleton, the corresponding problem becomes the weighted sum rate maximization. Furthermore, it is found that under such general secrecy rate objective function, the secrecy outage constraint can be tackled without approximation. This results in tightly realized target probability, which in turns leave more resource for further optimizing the secrecy rate.

To accommodate various sensing performance constraints in a unified way, we introduce a penalty variable and move the sensing constraint to the objective function. In addition to facilitating subsequent algorithm derivation, with the sensing constraint moved to the objective function, the feasible region is enlarged and better iteration trajectories are expected to be found. This is verified theoretically that the transformed problem share the same optimal solution as in the original problem with explicit sensing constraint, and a stationary point of the former must be at least a stationary point of the latter.

After the above transformation, since the remaining constraints are decoupled in the optimization variables, we further propose a projected gradient based alternative optimization (AO) with its solution quality guarantee theoretically proved. The advantage of the proposed unified framework is that when the sensing metric or objective function changes, only the gradient of the sensing metric or the projection of the auxiliary variables needs to be modified, rather than redesigning the whole algorithm. Leveraging the highly efficient gradient descent under simple constraints, the proposed method maintains a low computational complexity in each iteration. Moreover, since the proposed algorithm is non-monotonic, it can traverse the valleys of the objective function’s rugged surface to discover better solutions. Simulation results show that the proposed framework outperforms other existing algorithms in both running time and optimized secrecy rate under various sensing metric settings.

The contributions of this paper are summarized as follows.

- 1) We propose a framework incorporating the redundant information technique and artificial noise to enhance security of ISAC under covert eavesdroppers. We only assume the knowledge of distribution of eavesdroppers’ channels, but not their realizations. This leads to an intricate trade-off between secrecy outage probability (SOP), secrecy rate optimization and sensing performance.
- 2) The proposed framework holistically maximizes the worst-case user secrecy rate and the sum secrecy rate across multiple users, with both cases subsumed within a unified objective function. Moreover, the framework accurately controls secrecy outage probabilities while accommodating a broad spectrum of sensing

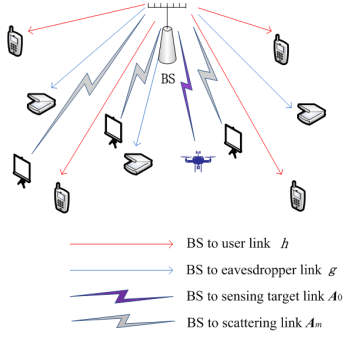


Fig. 1. Secure ISAC network model

constraints.

- 3) Unlike traditional approaches that rely on convex relaxation to handle sensing constraints, we propose a gradient-based iterative algorithm. This method leverages gradient information, combined with bisection methods and projection operations, to achieve fast convergence. Additionally, we theoretically establish the solution quality of the proposed algorithm.
- 4) We demonstrate the proposed unified framework with three different ISAC constraints as examples. Extensive simulation results show that the proposed framework consistently achieves higher optimized secrecy rates under various sensing constraints compared to existing methods. These results underscore its superiority and versatility in secure ISAC systems.

The rest of the paper is organized as follows. The secure ISAC system model is introduced and the worst user secrecy rate maximization is formulated in Section II. The problem formulation is generalized to unify worst user rate maximization and sum rate maximization under various sensing metrics in Section III. The proposed optimization framework and its solution quality analysis are presented in Section IV. The specific computation steps of the proposed framework under different sensing metrics are derived in Section V. Simulation results are provided in Section VI and conclusions are drawn in Section VII.

Notation: Symbols for vectors (lower case) and matrices (upper case) are presented in boldface. The transpose and conjugate transpose of a matrix are denoted by $(\cdot)^T$ and $(\cdot)^H$, respectively. The notation $\|\cdot\|_2$ represents the L2 norm of a vector, while \mathbf{I}_N is the identity matrix with dimension $N \times N$. A complex-valued vector $\mathbf{x} \sim \mathcal{CN}(\mathbf{0}, \mathbf{C})$ means \mathbf{x} is complex Gaussian distributed with zero mean and covariance matrix \mathbf{C} .

II. System Model and worst user secrecy rate maximization

We consider a ISAC network with a BS equipped with N antennas as shown in Fig. 1. The system includes I communication users, J eavesdroppers, each with a single antenna, and the channels from the BS to the i^{th} user and the j^{th} eavesdropper are denoted by $\mathbf{h}_i \in \mathbb{C}^{N \times 1}$ and $\mathbf{g}_j \in \mathbb{C}^{N \times 1}$, respectively. Besides, this network has a sensing target and M scatterings. In practice, the BS only has

knowledge $\mathbf{g}_j \sim \mathcal{CN}(\mathbf{0}, \rho_j^2 \mathbf{I}_N)$, but not the exact value of \mathbf{g}_j . The ρ_j here represents the large-scale fading coefficient of the j^{th} eavesdropper and it could be known if we know its approximate location. This assumption is commonly used in PLS to model the passive eavesdropping channels [20]–[23]. Furthermore, to avoid electromagnetic coupling, the transmit antennas are typically spaced by at least half a wavelength. Therefore, the signal paths arriving at or leaving from each antenna have negligible correlation, which leads to 0 in the off-diagonal elements of the channel covariance matrix. On the other hand, the assumption of the same diagonal elements of the covariance matrix is often valid when the BS is equipped with a uniform linear array (ULA) or uniform planar array (UPA), where all antennas have the same characteristics and are spaced symmetrically [40]. The above deployment ensures that no single antenna consistently experiences a stronger average signal than the others.

Let $s_i \in \mathbb{C}$ be the information symbol intended for the i^{th} user, with $s_i \sim \mathcal{CN}(0, 1)$ and is independent among users. With the beamforming vectors $\{\mathbf{w}_i\}_{i=1}^I$ for communication, artificial beamformer \mathbf{w}_0 and corresponding AN $s_0 \sim \mathcal{CN}(0, 1)$ for sensing and countering eavesdroppers, the transmitted signal of the BS is given by $\sum_{l=1}^I \mathbf{w}_l s_l + \mathbf{w}_0 s_0$. Correspondingly, the received signals at the i^{th} user and the j^{th} Eve are respectively given by

$$y_i = \mathbf{h}_i^T (\sum_{l=1}^I \mathbf{w}_l s_l + \mathbf{w}_0 s_0) + n_i, \quad (1)$$

$$e_j = \mathbf{g}_j^T (\sum_{l=1}^I \mathbf{w}_l s_l + \mathbf{w}_0 s_0) + \tilde{n}_j, \quad (2)$$

where $n_i \sim \mathcal{CN}(0, \sigma_i^2)$ and $\tilde{n}_j \sim \mathcal{CN}(0, \zeta_j^2)$ represent the Gaussian noises at the i^{th} user and the j^{th} Eve with variance σ_i^2 and ζ_j^2 , respectively.

Moreover, the echo signal received at the BS from the sensing target and scatterings is given by

$$\mathbf{r} = \sum_{m=0}^M \mathbf{A}_m (\sum_{l=1}^I \mathbf{w}_l s_l + \mathbf{w}_0 s_0) + \mathbf{n}_{BS}, \quad (3)$$

where $\mathbf{n}_{BS} \sim \mathcal{CN}(0, \sigma_{BS}^2 \mathbf{I}_N)$ represents the Gaussian noises at the BS with variance σ_{BS}^2 , $\{\mathbf{A}_m\}_{m=0}^M$ are the sensing channels of the target (\mathbf{A}_0) and scatterings $\{\mathbf{A}_m\}_{m \neq 0}$. In particular, $\mathbf{A}_m = \beta_m \mathbf{a}(\theta_m) \mathbf{a}^H(\theta_m)$, where β_m is the round-trip channel coefficient including the path loss and the radar cross-section (RCS) for the target ($m=0$) or scatterings ($m \neq 0$), and

$$\mathbf{a}(\theta_m) = [1, e^{j2\pi\zeta \sin \theta_m}, \dots, e^{j2\pi(N-1)\zeta \sin \theta_m}]^T \quad (4)$$

is the array steering vector of the BS with the angle from the BS to the sensing target denoted as θ_0 and that to the m^{th} scattering given by θ_m . The symbol ζ is the adjacent antennas spacing at the BS normalized by the wavelength [41]. Note that the channels \mathbf{h}_i , \mathbf{A}_0 are estimated in the pilot transmission phase [42], [43] and the scattering channels $\{\mathbf{A}_m\}_{m \neq 0}$ in the environment can be estimated based on field measurements or radio maps [44], [45].

With a receive filter $\mathbf{u} \in \mathbb{C}^{N \times 1}$ adopted at the BS, the

sensing SINR at the BS is

$$\gamma_{Rad} = \frac{\sum_{l=0}^I |\mathbf{u}^T \mathbf{A}_0 \mathbf{w}_l|^2}{\sum_{l=0}^I \sum_{m=1}^M |\mathbf{u}^T \mathbf{A}_m \mathbf{w}_l|^2 + \sigma_{BS}^2 \|\mathbf{u}\|_2^2}. \quad (5)$$

On the other hand, the achievable rate of the j^{th} Eve for monitoring the i^{th} user (also known as the eavesdropping rate) is given by

$$C_{ji} = \log_2 \left(1 + \frac{|\mathbf{g}_j^T \mathbf{w}_i|^2}{\sum_{l=0, l \neq i}^I |\mathbf{g}_j^T \mathbf{w}_l|^2 + \zeta_j^2} \right). \quad (6)$$

Since the BS does not have perfect knowledge of the eavesdroppers' channels, the value of C_{ji} is uncertain from the perspective of the BS. Consequently, a secrecy outage event occurs at the BSs when C_{ji} exceeds the redundancy rate of the i^{th} user, denoted by D_{ji} , and SOP of the user i due to Eve j is expressed as

$$\text{SOP} : p_{ji}^{so} = \Pr \{D_{ji} \leq C_{ji}\}. \quad (7)$$

Our objective is to maximize the secrecy rate of the worst communication user while maintaining the secrecy outage probability and the sensing performance of the target. Correspondingly, the optimization problem is formulated as

$$\max_{\{\mathbf{w}_l\}_{l=0}^I, \{D_{ji}\}, \mathbf{u}} \min_{j, i} \{ \mathcal{R}_i(\{\mathbf{w}_l\}_{l=0}^I) - D_{ji} \} \quad (8a)$$

$$\text{s.t. } p_{ji}^{so} \leq \eta_i, \quad \forall j, i \quad (8b)$$

$$\sum_{l=0}^I \|\mathbf{w}_l\|_2^2 \leq P_{BS}, \quad (8c)$$

$$\gamma_{Rad} \geq \Gamma, \quad (8d)$$

where $\mathcal{R}_i(\{\mathbf{w}_l\}_{l=0}^I) = \log_2 \left(1 + \frac{|\mathbf{h}_i^T \mathbf{w}_i|^2}{\sum_{l=0, l \neq i}^I |\mathbf{h}_i^T \mathbf{w}_l|^2 + \sigma_i^2} \right)$.

Constraint (8b) states that the secrecy outage probability of the i^{th} user monitored by the j^{th} eavesdropper should be smaller than a target threshold $\eta_i \in (0, 1)$. Constraint (8c) is the total power budget of the BS and (8d) requires the sensing SINR to be at least Γ to guarantee sensing performance. Notice that the SOP constraint (8b) is related to the beamformers inside the probability function. But the following lemma could be adopted to convert it into a deterministic form.

Lemma 1. [46, Lem 2] Suppose $\mathbf{g}_j \sim \mathcal{CN}(\mathbf{0}, \rho_j^2 \mathbf{I}_N)$, $\forall j$, the SOP constraint (8b) can be equivalently transformed into

$$\begin{aligned} & \ln \eta_i + \frac{(2^{D_{ji}} - 1)}{(\rho_j^2 / \zeta_j^2) \|\mathbf{w}_i\|_2^2} + \sum_{l=0, l \neq i}^I \ln \left(1 + (2^{D_{ji}} - 1) \frac{\|\mathbf{w}_l\|_2^2}{\|\mathbf{w}_i\|_2^2} \right) \\ & \geq 0, \end{aligned} \quad (9)$$

where ρ_j^2 / ζ_j^2 is interpreted as the statistical signal-to-noise ratio (SNR) for the j^{th} eavesdropper.

Although the probability constraint (8b) can be equivalently converted into a deterministic form in (9), it is still complex since the beamformers are coupled in a logarithm and fraction form. To handle this transformed SOP

constraint, [47]–[49] introduce $J \times I$ auxiliary constraints for substituting $(2^{D_{ji}} - 1) / \|\mathbf{w}_i\|_2^2$ with a new auxiliary variable t_{ji} and then use SCA to convexify all these introduced constraints. Another work [6] uses the matrix form of the beamformers $\mathbf{W}_i = \mathbf{w}_i \mathbf{w}_i^H$, and converts all the quadratic term $\|\mathbf{w}_l\|_2^2$ as a linear combination of $\text{Tr}(\mathbf{W}_l)$. Then, SDR can be adopted through further introducing convexified auxiliary constraints and temporarily discarding the rank-1 constraint. In general, these existing approaches involve exchanging (9) for a series of simpler, though more conservative, convexified constraints. Unfortunately, this often results in allocating limited resources to merely surpass the target outage probability, rather than optimizing the objective function [50].

To this end, we introduce a method for handling (9) without approximation or relaxation, thus tightly realize the target outage probability. In particular, it is recognized that the left hand side of (9) is a monotonic increasing function of D_{ji} . On the other hand, to maximize the secrecy rate (8a), D_{ji} should be minimized. Therefore, the optimal value of D_{ji} that maximizes the secrecy rate while maintaining the SOP constraint is given by (9) with equality holds. As a result, the optimal D_{ji} can be found by the bisection method when $\{\mathbf{w}_l\}_{l=0}^I$ are fixed. By denoting D_{ji} as $D_{ji}(\{\mathbf{w}_l\}_{l=0}^I)$, problem (8) becomes

$$\begin{aligned} & \max_{\{\mathbf{w}_l\}_{l=0}^I, \mathbf{u}} \min_i \{ \mathcal{R}_i(\{\mathbf{w}_l\}_{l=0}^I) - \max_j D_{ji}(\{\mathbf{w}_l\}_{l=0}^I) \} \\ & \text{s.t. } \sum_{l=0}^I \|\mathbf{w}_l\|_2^2 \leq P_{BS}, \\ & \quad \gamma_{Rad} \geq \Gamma. \end{aligned} \quad (10)$$

From (10), it is clear that the beamformers serve both purposes of enhancing security and target sensing. It can be anticipated that a higher sensing SINR requirement Γ would decrease the secrecy rate, and vice versa.

Through expressing D_{ji} as an implicit function of beamformers $\{\mathbf{w}_l\}_{l=0}^I$, the SOP constraint does not explicitly appear in (10). Since the optimal $D_{ji}(\{\mathbf{w}_l\}_{l=0}^I)$ is given by (9) with equality holds, a large ρ_j^2 / ζ_j^2 would result in a large redundancy rate $D_{ji}(\{\mathbf{w}_l\}_{l=0}^I)$. Therefore, the largest redundancy rate $D_i(\{\mathbf{w}_l\}_{l=0}^I) := \max_j \{D_{ji}(\{\mathbf{w}_l\}_{l=0}^I)\}$ of user i due to all eavesdroppers satisfies

$$\begin{aligned} & \ln \eta_i + \left(2^{D_i(\{\mathbf{w}_l\}_{l=0}^I)} - 1 \right) / \left[\max_j (\rho_j^2 / \zeta_j^2) \|\mathbf{w}_i\|_2^2 \right] \\ & + \sum_{l=0, l \neq i}^I \ln \left(1 + \left(2^{D_i(\{\mathbf{w}_l\}_{l=0}^I)} - 1 \right) \frac{\|\mathbf{w}_l\|_2^2}{\|\mathbf{w}_i\|_2^2} \right) = 0, \end{aligned} \quad (11)$$

which coincides with the intuition that the eavesdropper with the highest statistical SNR is the one that determines what redundancy rate a user needs in order to maintain the outage probability. Then problem (10) can be simpli-

fixed as

$$\max_{\{\mathbf{w}_l\}_{l=0}^I, \mathbf{u}} \min_i \left\{ \mathcal{R}_i(\{\mathbf{w}_l\}_{l=0}^I) - D_i(\{\mathbf{w}_l\}_{l=0}^I) \right\} \quad (12a)$$

$$s.t. \quad \sum_{l=0}^I \|\mathbf{w}_l\|_2^2 \leq P_{BS}, \quad (12b)$$

$$\gamma_{Rad} \geq \Gamma. \quad (12c)$$

According to the formulation of sensing SINR (5), the amplitude of the receive filter \mathbf{u} does not affect the value of γ_{rad} , therefore, the sensing constraint (12c) can be equivalently transformed into

$$\sum_{l=0}^I |\mathbf{u}^T \mathbf{A}_0 \mathbf{w}_l|_2^2 - \Gamma \sum_{l=0}^I \sum_{m=1}^M |\mathbf{u}^T \mathbf{A}_m \mathbf{w}_l|_2^2 - \Gamma \sigma_{BS}^2 \geq 0, \quad (13a)$$

$$\|\mathbf{u}\|_2^2 = 1. \quad (13b)$$

Hence, the worst case secrecy rate maximization under sensing SINR constraint is equivalent to

$$\max_{\{\mathbf{w}_l\}_{l=0}^I, \mathbf{u}} \min_i \left\{ \mathcal{R}_i(\{\mathbf{w}_l\}_{l=0}^I) - D_i(\{\mathbf{w}_l\}_{l=0}^I) \right\} \quad (14a)$$

$$s.t. \quad \sum_{l=0}^I \|\mathbf{w}_l\|_2^2 \leq P_{BS}, \quad (14b)$$

(13a), (13b).

It is emphasized that (14) covers the common worst user's achievable rate maximization if eavesdroppers do not exist, which corresponds to $D_i(\{\mathbf{w}_l\}_{l=0}^I) \equiv 0$. Moreover, in ISAC, there exists sensing performance criteria other than SINR constraint. The above two observations inspire us to extend (14) in the following section.

Remark 1 (SOP vs intercept probability): Beside SOP, another commonly used outage probability is the intercept probability [51], [52], which is given by

$$\Pr \left\{ \mathcal{R}_i(\{\mathbf{w}_l\}_{l=0}^I) \leq C_{ji} \right\}. \quad (15)$$

It is a metric to quantify the likelihood of a successful interception of the entire information transmitted with $\mathcal{R}_i(\{\mathbf{w}_l\}_{l=0}^I)$. On the other hand, SOP in (7) measures the probability of the information leakage of the i^{th} user. When the eavesdropping rate C_{ji} exceeds the redundant information D_{ji} , it means the confidentiality of the transmitted information cannot be guaranteed. However, it is important to note that information leakage does not necessarily mean that all useful information has been intercepted by the eavesdroppers. In general, since D_{ji} is the amount of redundant information added to a message to secure it from eavesdroppers, $\mathcal{R}_i(\{\mathbf{w}_l\}_{l=0}^I) > D_{ji}$, which makes

$$\Pr \{D_{ji} \leq C_{ji}\} \geq \Pr \left\{ \mathcal{R}_i(\{\mathbf{w}_l\}_{l=0}^I) \leq C_{ji} \right\}. \quad (16)$$

The implication of (16) is that imposing constraint on SOP would also restrict intercept probability. In another perspective, SOP provides a more stringent measure of security. Together with the fact that employing redundant information is a common strategy in secure and covert transmission [53]–[57], our primary focus is on the SOP.

III. Extension to general sensing constraint in ISAC

As the sensing target and the scatterings are not directly related to the communication users and eavesdroppers, with the introduction of auxiliary variables $\{y_i\}_{i=1}^I$, we can extend (14) to a generalized rate optimization in ISAC:

$$\max_{\{\mathbf{w}_l\}_{l=0}^I, \mathbf{v}} \min_{\{y_i\}_{i=1}^I} \sum_{i=1}^I y_i \psi_i(\{\mathbf{w}_l\}_{l=0}^I) \quad (17a)$$

$$s.t. \quad \sum_{l=0}^I \|\mathbf{w}_l\|_2^2 \leq P_{BS}, \quad (17b)$$

$$S(\{\mathbf{w}_l\}_{l=0}^I, \mathbf{v}) \geq 0, \quad (17c)$$

$$\mathbf{v} \in \Omega_{\mathbf{v}}, \quad (17d)$$

$$\{y_i\} \in \Omega_{\mathbf{y}}, \quad (17e)$$

where $\psi_i(\{\mathbf{w}_l\}_{l=0}^I)$ could be the secrecy rate $\mathcal{R}_i(\{\mathbf{w}_l\}_{l=0}^I) - D_i(\{\mathbf{w}_l\}_{l=0}^I)$ if eavesdroppers are present or the achievable rate $\mathcal{R}_i(\{\mathbf{w}_l\}_{l=0}^I)$ if there is no eavesdropper, $S(\{\mathbf{w}_l\}_{l=0}^I, \mathbf{v})$ is the sensing performance metric of interest, \mathbf{v} contains other optimization variables related to the sensing performance and $\Omega_{\mathbf{v}}$ is the feasible region of \mathbf{v} . Furthermore, $\Omega_{\mathbf{y}}$ is the feasible set of the auxiliary variables $\{y_i\}_{i=1}^I$. Without loss of generality, we assume that $\{\psi_i(\{\mathbf{w}_l\}_{l=0}^I)\}_{i=1}^I$ and $S(\{\mathbf{w}_l\}_{l=0}^I, \mathbf{v})$ are twice differentiable.

Problem (17) covers two widely used objective functions. **Objective 1: Worst user secrecy rate.** In the case, the constraint on \mathbf{y} is a simplex $\Omega_{\mathbf{y}} := \{\sum_{i=1}^I y_i = 1, y_i \geq 0, \forall i\}$. In order to minimize the summation of the rates under this $\Omega_{\mathbf{y}}$, the inner minimization with respect to (w.r.t.) $\{y_i\}$ would allocate zero to the non-minimal rates and one to the minimal rate so that the summation of rates would reach its minimal solution, i.e., $\min_i \psi_i(\{\mathbf{w}_l\}_{l=0}^I)$ as in worst case rate maximization (14). An advantage of the formulation (17) under simplex constraint of $\{y_i\}_{i=1}^I$ over the worst user rate maximization (14) is that the inner minimization is changed from a discrete user selection problem into a minimization problem with continuous variables $\{y_i\}$, which allows a continuous iteration of these variables (more details will be presented in the next section).

Objective 2: Weighted sum secrecy rate. In this case, $\Omega_{\mathbf{y}} := \{y_i = \tilde{y}_i, \forall i\}$ is a singleton set. Then the inner minimization w.r.t. $\{y_i\}$ in (17) can be skipped. As a special case, when $\tilde{y}_i = 1$ for all i , it becomes the sum rate maximization problem. Also, if \tilde{y}_i is one for one user and zero for other users, problem (17) would turn into rate maximization of a single user. This makes (17a) a generalization to include both worst user rate maximization and weighted sum rate maximization for the communication users. Notice that since SOP constraint does not explicitly appear in (17), for an ISAC system without eavesdroppers, $\psi_i(\{\mathbf{w}_l\}_{l=0}^I)$ can be any utility beyond the secrecy rate and achievable rate. However, since we focus on secure ISAC, we do not pursue this direction further in this paper.

Formulation (17) not only extends the objective function but also generalizes the sensing metric. While our goal is not to exhaustively list all possible sensing criteria, below are a few popular sensing metrics used in existing research. Metric 1: Sensing SINR. This is the case we discussed in Section II. Correspondingly, $S(\{\mathbf{w}_l\}_{l=0}^I, \mathbf{v})$ is given by the left hand side of (13a) with $\mathbf{v} = \mathbf{u}$ and $\Omega_{\mathbf{v}}$ is the feasible region given by the constraint (13b).

Metric 2: Beampattern matching. The mean squared error (MSE) between the sensing beampattern and the ideal beampattern can be employed as a sensing criterion, which is written as [14], [58]

$$\begin{aligned} MSE(\{\mathbf{w}_l\}_{l=0}^I) &= \frac{1}{T} \sum_{t=1}^T \left| P_d(\theta_t) - \mathbf{a}^H(\theta_t) \left(\sum_{l=0}^I \mathbf{w}_l \mathbf{w}_l^H \right) \mathbf{a}(\theta_t) \right|^2, \end{aligned} \quad (18)$$

where T represents the number of sampling angles, $P_d(\theta_t)$ is the desired beampattern at the target angle θ_t and $\mathbf{a}(\theta_t)$ is given in (4). Correspondingly, the sensing performance constraint is written as

$$MSE(\{\mathbf{w}_l\}_{l=0}^I) \leq \gamma, \quad (19)$$

where γ is the allowable MSE. In this case, $S(\{\mathbf{w}_l\}_{l=0}^I) = \gamma - MSE(\{\mathbf{w}_l\}_{l=0}^I)$ and $\Omega_{\mathbf{v}} = \emptyset$.

Metric 3: Detection probability. It is known that with the receive filter $\mathbf{u} \in \mathbb{C}^{N \times 1}$ orthogonal to the steering vectors $\{\mathbf{a}(\theta_m)\}_{m \neq 0}$ of all scatterings, the interferences from the scatterings can be suppressed. With the derivations in [59], the detection probability P_D of the sensing target for a given false-alarm probability P_{FA} is given by

$$P_D = Q \left(Q^{-1}(P_{FA}) - \sqrt{\frac{2\beta_0^2 \mathbf{a}^H(\theta_0) \left(\sum_{l=0}^I \mathbf{w}_l \mathbf{w}_l^H \right) \mathbf{a}(\theta_0)}{\sigma_{BS}^2}} \right), \quad (20)$$

where $Q(\cdot)$ is the right-tailed distribution function of the standard Gaussian distribution and $Q^{-1}(\cdot)$ is its inverse function. To maintain a target detection probability ϕ , we need

$$P_D \geq \phi. \quad (21)$$

Based on (20), constraint (21) can be reformulated as

$$\sum_{l=0}^I \mathbf{w}_l^H \mathbf{A}_0 \mathbf{w}_l - [\sigma_{BS}^2 (Q^{-1}(P_{FA}) - Q^{-1}(\phi)) / 2\beta_0] \geq 0, \quad (22)$$

where \mathbf{A}_0 is defined in (3). In this case, $S(\{\mathbf{w}_l\}_{l=0}^I)$ is given by the left hand side of (22) and $\Omega_{\mathbf{v}} = \emptyset$.

Remark 2 (Generality of (17) without eavesdroppers): The problem formulation (17) and thus the subsequent proposed algorithm also cover the cases of worst user sum rate and weighted user sum rate maximization without eavesdroppers. This can be easily achieved by setting $\eta_i = 1$ in the SOP constraint, which will automatically lead to

$D_i(\{\mathbf{w}_l\}_{l=0}^I) = 0$ in (11). While this case is not the focus of this paper as no PLS is provided, the developed framework also unifies the treatment of ordinary ISAC under various sensing constraints.

IV. Proposed framework for solving the general max-min problem (17)

Since (17) includes worst user rate or sum rate in the objective and various sensing metrics in the constraint as special cases, it is desirable to have a unified framework for solving it. For tackling the general max-min formulation (17), existing methods would firstly transform the max-min into a pure maximization problem, either through introducing a single auxiliary variable to replace the inner minimization in the objective function and then put the inner minimization as constraints [41], [60], [61], or using the penalty reformulation [47]. In general, these methods either face difficulty in setting an appropriate objective function for the outer layer variables [62], or losing the solution quality guarantee due to manually tuning of penalty parameter.

Furthermore, the generally non-convex or even highly complex $S(\{\mathbf{w}_l\}_{l=0}^I, \mathbf{v})$ in the constraint is another challenge in handling (17). Existing dominant methods for handling a non-convex constraint $S(\{\mathbf{w}_l\}_{l=0}^I, \mathbf{v})$ would involve convexifying it. However, since the sensing constraint in (17) is in a general form, common tactics such as Taylor expansion or semidefinite relaxation for quadratic constraint may not be applicable. For example, for the beampattern matching constraint, it is not quadratic in $\{\mathbf{w}_l\}_{l=0}^I$. In this case, we need to introduce additional conservative auxiliary constraints, which tightens the feasible region and loses convergence points in the excluded region. To develop a solution for the general problem, we will handle the inner minimization and the constraint $S(\{\mathbf{w}_l\}_{l=0}^I, \mathbf{v})$ at the same time below.

More specifically, rewriting the auxiliary variables $\{y_i\}_{i=1}^I$ as a vector $\mathbf{y} := [y_1, y_2, \dots, y_I]^T$ and introducing one more non-negative penalty variable c , (17) can be converted to

$$\max_{\{\mathbf{w}_l\}_{l=0}^I, \mathbf{v}} \min_{c, \mathbf{y}} \mathbf{y}^T \boldsymbol{\psi}(\{\mathbf{w}_l\}_{l=0}^I) + cS(\{\mathbf{w}_l\}_{l=0}^I, \mathbf{v}) \quad (23a)$$

$$\text{s.t.} \quad \sum_{l=0}^I \|\mathbf{w}_l\|_2^2 \leq P_{BS}, \quad (23b)$$

$$\mathbf{v} \in \Omega_{\mathbf{v}}, \quad (23c)$$

$$\mathbf{y} \in \Omega_{\mathbf{y}}, \quad (23d)$$

$$c \geq 0, \quad (23e)$$

where $\boldsymbol{\psi}(\{\mathbf{w}_l\}_{l=0}^I) = [\psi_1(\{\mathbf{w}_l\}_{l=0}^I), \dots, \psi_I(\{\mathbf{w}_l\}_{l=0}^I)]^T$ is a column vector containing the utilities of all users. The solution equivalence between (17) and (23) is given in the following Proposition.

Proposition 1. If $\{\{\hat{\mathbf{w}}_l\}_{l=0}^I, \hat{\mathbf{v}}, \hat{\mathbf{y}}, \hat{c}\}$ is the optimal solution of (23), then $\{\{\hat{\mathbf{w}}_l\}_{l=0}^I, \hat{\mathbf{v}}, \hat{\mathbf{y}}\}$ is the optimal solution of (17). Conversely, if $\{\{\hat{\mathbf{w}}_l\}_{l=0}^I, \hat{\mathbf{v}}, \hat{\mathbf{y}}\}$ is the optimal solution of (17), then $\{\{\hat{\mathbf{w}}_l\}_{l=0}^I, \hat{\mathbf{v}}, \hat{\mathbf{y}}, \hat{c} = 0\}$ is the optimal

solution of (23). Furthermore, if $\{\{\mathbf{w}_l^*\}_{l=0}^I, \mathbf{v}^*, \mathbf{y}^*, c^*\}$ is a stationary point of (23), $\{\{\mathbf{w}_l^*\}_{l=0}^I, \mathbf{v}^*, \hat{\mathbf{y}}^*\}$ is at least a stationary point of (17).

Proof: Due to page limitation, we only provide a sketch of the proof in the following. More details can be found in Appendix A in supplementary material. First, it can be proved that the optimal solution of (23) must have $\hat{c}S(\{\hat{\mathbf{w}}_l\}_{l=0}^I, \hat{\mathbf{v}}) = 0$ and $S(\{\hat{\mathbf{w}}_l\}_{l=0}^I, \hat{\mathbf{v}}) \geq 0$. This causes the term $cS(\{\mathbf{w}_l\}_{l=0}^I, \mathbf{v})$ vanishes at the optimal solution of (23) and makes it equivalent to (17). Second, if $\{\{\mathbf{w}_l^*\}_{l=0}^I, \mathbf{v}^*, \hat{\mathbf{y}}^*, c^*\}$ is the stationary point of (23) but $\{\{\mathbf{w}_l^*\}_{l=0}^I, \mathbf{v}^*, \hat{\mathbf{y}}^*\}$ is not a stationary point of (17), we can construct a sequence gradually approaching $\{\{\mathbf{w}_l^*\}_{l=0}^I, \mathbf{v}^*, \hat{\mathbf{y}}^*\}$ and always violates the sensing metric constraint when the points in this sequence is sufficiently close to $\{\{\mathbf{w}_l^*\}_{l=0}^I, \mathbf{v}^*, \hat{\mathbf{y}}^*\}$. In this way, we can prove that $\{\{\mathbf{w}_l^*\}_{l=0}^I, \mathbf{v}^*, \hat{\mathbf{y}}^*, c^*\}$ is not a stationary point of (23). By contradiction, the second part is proved. \square

Through moving the sensing constraint into the objective function, the functions $\psi(\{\mathbf{w}_l\}_{l=0}^I)$ and $S(\{\mathbf{w}_l\}_{l=0}^I, \mathbf{v})$ only exist in the objective function and the constraints become much simpler. Moreover, as \mathbf{y} and c are continuous variables, an intuitive approach for solving (23) is to use AO between the inner minimization and the outer maximization. Specifically, at the k^{th} iteration, given the current iteration point $\{\{\mathbf{w}_l^k\}_{l=0}^I, \mathbf{v}^k, c^k, \mathbf{y}^k\}$, we alternatively solve the following two subproblems

$$\begin{aligned} \{c^{k+1}, \mathbf{y}^{k+1}\} = \arg \min_{c, \mathbf{y}} & \mathbf{y}^T \psi(\{\mathbf{w}_l^k\}_{l=0}^I) \\ & + cS(\{\mathbf{w}_l^k\}_{l=0}^I, \mathbf{v}^k) \quad (24) \\ \text{s.t. } & \mathbf{y} \in \Omega_{\mathbf{y}}, c \geq 0. \end{aligned}$$

$$\begin{aligned} \{\{\mathbf{w}_l^{k+1}\}_{l=0}^I, \mathbf{v}^{k+1}\} = \arg \max_{\{\mathbf{w}_l\}_{l=0}^I, \mathbf{v}} & (\mathbf{y}^{k+1})^T \psi(\{\mathbf{w}_l\}_{l=0}^I) \\ & + c^{k+1}S(\{\mathbf{w}_l\}_{l=0}^I, \mathbf{v}) \\ \text{s.t. } & \sum_{l=0}^I \|\mathbf{w}_l\|_2^2 \leq P_{BS}, \\ & \mathbf{v} \in \Omega_{\mathbf{v}}. \quad (25) \end{aligned}$$

Unfortunately, alternatively solving the above two subproblems is not a viable solution. In particular, notice that the objective function in (24) is linear w.r.t. c . Given that the constraint $c \geq 0$ is an unbounded set and $S(\{\mathbf{w}_l\}_{l=0}^I, \mathbf{v})$ can be negative before convergence, the solution of c in (24) could be unbounded, which could block subsequent iterations. Furthermore, since the minimization problem (24) is a strictly linear function of \mathbf{y} , the optimal solution w.r.t. \mathbf{y} may not be unique for the general feasible set $\Omega_{\mathbf{y}}$ (e.g., $\Omega_{\mathbf{y}}$ under worst case rate optimization problem with two or more users having the same minimal rate in $\psi(\{\mathbf{w}_l^k\}_{l=0}^I)$). Randomly choosing one from the solution set would make the solution sequence has a sudden jump, which imposes challenges to the solution quality analysis. To avoid an unbounded iterate

c^k and handle the non-uniqueness of \mathbf{y}^k , the subproblem for inner minimization should be modified.

A. Regularizing the inner minimization problem

To deal with the possible unbounded iterate of c and non-unique solution of \mathbf{y} at the k^{th} iteration, we propose to modify (24) as the following regularized minimization problem

$$\begin{aligned} \{c^{k+1}, \mathbf{y}^{k+1}\} = \arg \min_{c, \mathbf{y}} & \mathbf{y}^T \psi(\{\mathbf{w}_l^k\}_{l=0}^I) + \frac{\lambda_{\mathbf{y}}^k}{2} \|\mathbf{y}\|_2^2 \\ & + cS(\{\mathbf{w}_l^k\}_{l=0}^I, \mathbf{v}^k) + \frac{\lambda_c^k}{2} c^2 + \frac{\beta^k}{2} (c - c^k)^2 \\ \text{s.t. } & \mathbf{y} \in \Omega_{\mathbf{y}}, \\ & c \in [0, C^k], \quad (26) \end{aligned}$$

where $\lambda_c^k, \lambda_{\mathbf{y}}^k, \beta^k, C^k$ are positive regularization parameters. The regularization term $\beta^k(c - c^k)^2/2$ ensures that the next iteration point c^{k+1} would not go far from the current point c^k . The term $\lambda_c^k c^2/2$ and C^k guarantees that the solution c^{k+1} of this inner minimization problem would not go to infinity and block the iteration. On the other hand, to make the solution of \mathbf{y} unique, we introduce a strongly convex term $\lambda_{\mathbf{y}}^k \|\mathbf{y}\|_2^2/2$. To ensure the subproblem (26) be consistent with the original subproblem (24) as the number of iteration increases, we impose $\lim_{k \rightarrow \infty} \lambda_{\mathbf{y}}^k = \lim_{k \rightarrow \infty} \lambda_c^k = \lim_{k \rightarrow \infty} \beta^k = 0$ and $\lim_{k \rightarrow \infty} C^k = \infty$. Although the non-uniqueness of \mathbf{y} might occur again when k goes to infinity, this does not matter in practice since the number of iteration would be stopped at a finite number. Obviously, the schedule of the regularization parameters $\lambda_{\mathbf{y}}^k, \lambda_c^k, \beta^k$ and C^k would affect the solution quality of the whole AO iteration. This issue will be analyzed in subsection IV-D.

B. Finding an ascent point for the outer maximization problem

Notice that the outer maximization w.r.t. $\{\{\mathbf{w}_l\}_{l=0}^I, \mathbf{v}\}$ involves the utility functions $\psi(\{\mathbf{w}_l\}_{l=0}^I)$ and a general sensing constraint $S(\{\mathbf{w}_l\}_{l=0}^I, \mathbf{v})$, which precludes the possibility of finding a general concave approximation [47], [63], [64] to the objective function in (25). Fortunately, since $\psi(\{\mathbf{w}_l\}_{l=0}^I)$ and $S(\{\mathbf{w}_l\}_{l=0}^I, \mathbf{v})$ are differentiable, their gradients can be obtained. Based on this observation, a simple projected gradient ascent (27) (shown at the top of next page) is adopted to find an ascent point, where $1/\alpha^k$ is an appropriately chosen stepsize.

According to [65], in order to ensure (27) is an ascent point of the original maximization subproblem (25), α^k in (27) should be larger than the Lipschitz constant of the objective function (25). Since the utility function $\psi(\{\mathbf{w}_l\}_{l=0}^I)$ and constraint $S(\{\mathbf{w}_l\}_{l=0}^I, \mathbf{v})$ are assumed to be twice continuously differentiable, the Lipschitz constant of the objective function (25) exists. However, in practice, the Lipschitz constant may be difficult to

$$\begin{aligned}
\left\{ \{\mathbf{w}_l^{k+1}\}_{l=0}^I, \mathbf{v}^{k+1} \right\} = \arg \min_{\{\mathbf{w}_l\}_{l=0}^I, \mathbf{v}} & \left\| \mathbf{w}_l - \left(\mathbf{w}_l^k + \frac{1}{\alpha^k} \left[(\mathbf{y}^{k+1})^T \nabla_{\mathbf{w}_l} \psi \left(\{\mathbf{w}_l^k\}_{l=0}^I \right) + c^{k+1} \nabla_{\mathbf{w}_l} S \left(\{\mathbf{w}_l^k\}_{l=0}^I, \mathbf{v}^k \right) \right] \right) \right\|_2^2 \\
& + \left\| \mathbf{v} - \left(\mathbf{v}^k + \frac{c^{k+1}}{\alpha^k} \nabla_{\mathbf{v}} S \left(\{\mathbf{w}_l^k\}_{l=0}^I, \mathbf{v}^k \right) \right) \right\|_2^2 \\
s.t. & \sum_{l=0}^I \|\mathbf{w}_l\|_2^2 \leq P_{BS}, \\
& \mathbf{v} \in \Omega_{\mathbf{v}}.
\end{aligned} \tag{27}$$

Algorithm 1 Modified AO iteration for solving (23)

Input:

The upper bound of the iteration numbers K

Output:

$\{\{\mathbf{w}_l^{best}\}_{l=0}^I, \mathbf{v}^{best}\}$

General step:

- 1: Initialize $\{\{\mathbf{w}_l^1\}_{l=0}^I, \mathbf{v}^1, c^1, \mathbf{y}^1\}$ as any feasible point of the problem (23). Set $\{\mathbf{w}_l^{best}\}_{l=0}^I \leftarrow \{\mathbf{w}_l^1\}_{l=0}^I$ and $\mathbf{v}^{best} \leftarrow \mathbf{v}^1$
 - 2: For $k = 1, 2, \dots, K$
 - 3: Calculate $\lambda_c^k, \lambda_{\mathbf{y}}^k, \beta^k, \alpha^k$ and C^k
 - 4: Obtain $\{c^{k+1}, \mathbf{y}^{k+1}\}$ by solving (26)
 - 5: Obtain $\{\{\mathbf{w}_l^{k+1}\}_{l=0}^I, \mathbf{v}^{k+1}\}$ by solving (27)
 - 6: If the current iteration solution $\{\{\mathbf{w}_l^{k+1}\}_{l=0}^I, \mathbf{v}^{k+1}\}$ satisfies $S(\{\mathbf{w}_l^{k+1}\}_{l=0}^I, \mathbf{v}^{k+1}) \geq 0, \mathbf{v}^{k+1} \in \Omega_{\mathbf{v}}$ and $\min_{\mathbf{y} \in \Omega_{\mathbf{y}}} \mathbf{y}^T \psi(\{\mathbf{w}_l^{k+1}\}_{l=0}^I) \geq \min_{\mathbf{y} \in \Omega_{\mathbf{y}}} \mathbf{y}^T \psi(\{\mathbf{w}_l^{best}\}_{l=0}^I)$
 - 7: $\{\mathbf{w}_l^{best}\}_{l=0}^I \leftarrow \{\mathbf{w}_l^{k+1}\}_{l=0}^I$ and $\mathbf{v}^{best} \leftarrow \mathbf{v}^{k+1}$
 - 8: End
 - 9: until the iteration number k meets the upper bound K .
-

find (e.g., when involving an implicit function such as $D_i(\{\mathbf{w}_l\}_{l=0}^I)$). Inspired by the diminishing stepsize rule in the projected gradient method [66], α^k can be chosen as an increasing sequence with $\lim_{k \rightarrow \infty} \alpha^k = \infty$. Then, as the iteration goes, α^k will eventually exceed the Lipschitz constant of (25) and guarantee to provide an ascent point of (25). Similar to the regularization parameters in the inner minimization subproblem, theoretical results on the schedule of α^k would be given later.

C. Overall modified AO algorithm

The overall proposed AO iteration for solving (23) is summarized in Algorithm 1. Notice that as this modified AO iteration involves two opposing layers, the objective value generated by the sequence $\{\{\mathbf{w}_l^k\}_{l=0}^I, \mathbf{v}^k, c^k, \mathbf{y}^k\}$ is not monotonic. Therefore, in Algorithm 1, we need steps 6 and 7 to keep track of the current best solution.

For the outer iteration, due to the general forms of $\psi(\{\mathbf{w}_l^k\}_{l=0}^I)$ and $S(\{\mathbf{w}_l\}_{l=0}^I, \mathbf{v})$, there is no guarantee we could obtain a suboptimal or stationary point of the

objective function (25) even we execute (27) for many iterations. Moreover, the max-min problem (23) involves a coupled structure where the inner minimization influences the outer maximization. Updating the outer variables multiple times before updating the inner variables can lead to a misalignment between the two layers, which causes the algorithm to spend unnecessary time adjusting the outer variables based on outdated or inconsistent inner solutions, effectively slowing down the convergence [67]. Therefore, we propose to execute (27) for only one iteration and then move to the inner minimization of $\{c, \mathbf{y}\}$ in (26). Although we only obtain an ascent point of (25) by a single iteration, solution quality of the whole AO iteration can still be obtained. This is because the convergence and solution quality depend on the stepsize and the weight of the introduced regularization terms [68]–[70] in (26). It does not rely on whether we use multiple projected gradient steps or single projected step in outer maximization layer. The detailed convergence analysis for the whole modified AO iteration will be provided next.

D. Solution quality analysis

Although there exist some solution quality analyses for algorithms solving non-concave convex max-min problems [67]–[72], they are not applicable to the proposed AO iteration for solving (23). Firstly, existing analyses are carried out for algorithms with known Lipschitz constant [67]–[70] or upper bound of the Hessian matrix norm [71] of the objective function (23a). Although the Lipschitz constant or upper bound of the Hessian matrix norm of (23a) exist since (23a) is twice continuously differentiable, the general form of function $\psi(\{\mathbf{w}_l\}_{l=0}^I)$ and sensing metric $S(\{\mathbf{w}_l\}_{l=0}^I, \mathbf{v})$ in (23a) make them unobtainable. Furthermore, the solution quality analyses of these existing works require the constraints of the max-min problem to be bounded [67], [72]. Unfortunately, this is not valid in our case since the constraint $c \geq 0$ of the auxiliary variable is obviously unbounded. Therefore, a dedicated analysis is needed for the proposed algorithm.

Before we reveal the solution quality guarantee of the algorithm, we need to define the ε -stationary point which is commonly used in the analysis of non-monotonic algorithms for solving max-min problem.

Definition 1. (ε -stationary point) [67, Def 3.1], [68, Def 3.1] Given a max-min problem $\max_{\mathbf{x} \in \mathcal{X}} \min_{\mathbf{z} \in \mathcal{Z}} f(\mathbf{x}, \mathbf{z})$, let $\mathbb{I}_{\mathcal{X}}(\mathbf{x})$ and $\mathbb{I}_{\mathcal{Z}}(\mathbf{z})$ be the indicator functions of the constraints $\mathbf{x} \in \mathcal{X}$ and $\mathbf{z} \in \mathcal{Z}$, respectively. We call $\{\mathbf{x}^k, \mathbf{z}^k\}$ is a ε -stationary point of this max-min problem if there exists $\mathbf{d} \in \partial \mathbb{I}_{\mathcal{X}}(\mathbf{x})$ and $\mathbf{e} \in \partial \mathbb{I}_{\mathcal{Z}}(\mathbf{z})$ such that $\left\| \begin{bmatrix} \nabla_{\mathbf{x}} f(\mathbf{x}, \mathbf{z}) - \mathbf{d} \\ \nabla_{\mathbf{z}} f(\mathbf{x}, \mathbf{z}) + \mathbf{e} \end{bmatrix} \right\|_2 \leq \varepsilon$, where ∂ is the subgradient operation on the non-smooth indicator functions.

Next we present the convergence and solution quality of Algorithm 1 in Proposition 2.

Proposition 2. Define $T(\varepsilon)$ as the iteration index of Algorithm 1 obtaining a ε -stationary point of (23) for the first time. Suppose the sensing metric $S(\{\mathbf{w}_l\}_{l=0}^I, \mathbf{v})$ and utility function $\psi(\{\mathbf{w}_l\}_{l=0}^I)$ are twice continuously differentiable and the feasible set $\Omega_{\mathbf{v}}$ is compact. Also, assume that the global optimal solution of (26) and (27) can be obtained. Then, an upper bound of $T(\varepsilon)$ is given by $T(\varepsilon) \leq \mathcal{O}(\varepsilon^{-6})$ under the setting $\lambda_c^k = \lambda_{\mathbf{y}}^k \propto k^{-\frac{1}{4}}$, $\beta^k \propto k^{-3}$, $\alpha^k \propto k^{\frac{1}{3}}$ and $C^k \propto \ln k$.

Proof: Due to page limitation, we only provide a sketch of the proof in the following. More details can be found in Appendix B in supplementary material. First, we can prove the smoothness of the regularized inner minimization subproblem (26) due to the twice continuously differentiable of $S(\{\mathbf{w}_l\}_{l=0}^I, \mathbf{v})$, $\psi(\{\mathbf{w}_l\}_{l=0}^I)$ and gradient consistence theory [73]. Second, we can prove the difference of the optimal objective value of the subproblem (26) between the iteration points $\{\{\mathbf{w}_l^{k+1}\}_{l=0}^I, \mathbf{v}^{k+1}\}$ and $\{\{\mathbf{w}_l^k\}_{l=0}^I, \mathbf{v}^k\}$ is lower bounded. Lastly, applying the definition of ε -stationary point and convergent Bertrand series [74], Proposition 2 is proved. \square

According to Proposition 2, the proposed algorithm can find at least one ε -stationary point of (23) within $\mathcal{O}(\varepsilon^{-6})$ iterations ($\mathcal{O}(\varepsilon^{-6})$ can be interpreted as a conservative convergence rate). This means that as the number of iteration k increases, we are guaranteed to find a ε -stationary point with ε arbitrarily close to zero, which corresponds to a stationary point of (23). According to Proposition 1, a stationary point of (23) is at least a stationary point of (17). Therefore, Algorithm 1 is guaranteed to give at least a stationary point of (17) as the number of iteration goes to infinity.

Regarding the compact set assumption in Proposition 2, as the wireless resources related to the variable \mathbf{v} should not be unlimited, the feasible set $\Omega_{\mathbf{v}}$ should be compact. On the other hand, Proposition 2 requires the global optimal solution of (26) and (27), which seems to be restrictive since the objective functions in (26) and (27) contain the general sensing performance metric $S(\{\mathbf{w}_l\}_{l=0}^I, \mathbf{u})$. But a closer look reveals that the sensing metrics in (26) and (27) only depend on the k^{th} iteration solution but not the unknown variables, making the objective functions of (26) and (27) only contain at most quadratic terms of the optimization variables. This makes

it possible to obtain the global optimal solutions of (26) and (27), which will be discussed in the next section.

V. Solving (26) and (27) under different ISAC sensing metrics

A. Obtaining the global optimal solution of (26)

Notice that \mathbf{y} and c are decoupled in both the objective function and the constraints in (26). This makes it possible to solve (26) by independently minimizing subproblems w.r.t. \mathbf{y} and c . The details are given as follows.

Updating \mathbf{y} : Focusing on the terms related to \mathbf{y} in (26), the problem becomes

$$\begin{aligned} \min_{\mathbf{y}} \quad & \mathbf{y}^T \boldsymbol{\psi} \left(\{\mathbf{w}_l^k\}_{l=0}^I \right) + \frac{\lambda_{\mathbf{y}}^k}{2} \|\mathbf{y}\|^2 \\ \text{s.t.} \quad & \mathbf{y} \in \Omega_{\mathbf{y}}. \end{aligned} \quad (28)$$

Since this is a projection problem with a quadratic objective function, the optimal solution is

$$\mathbf{y}^{k+1} = \text{Proj}_{\Omega_{\mathbf{y}}} \left(-\frac{\boldsymbol{\psi} \left(\{\mathbf{w}_l^k\}_{l=0}^I \right)}{\lambda_{\mathbf{y}}^k} \right), \quad (29)$$

where $\text{Proj}_{\mathcal{A}}(b)$ is to project b to the feasible set \mathcal{A} . If the constraint on \mathbf{y} is a singleton, \mathbf{y} is a constant and (28) can be skipped. In the worst utility maximization, $\Omega_{\mathbf{y}} := \{\sum_{i=1}^I y_i = 1, y_i \geq 0, \forall i\}$, and (29) under such constraint can be obtained as [75]

$$\mathbf{y}^{k+1}(\iota) = \left[-\frac{\boldsymbol{\psi}(\{\mathbf{w}_l^k\}_{l=0}^I) + \iota}{\lambda_{\mathbf{y}}^k} \right]^+, \quad (30)$$

where ι satisfies $\mathbf{1}^T \mathbf{y}^{k+1}(\iota) = 1$ and can be found by the bisection method from the interval $[\min_i \{-\psi_i(\{\mathbf{w}_l^k\}_{l=0}^I)\} - \lambda_{\mathbf{y}}^k, \max_i \{-\psi_i(\{\mathbf{w}_l^k\}_{l=0}^I)\}]$.

Updating c : Focusing on the terms related to c in (26), the problem becomes

$$\begin{aligned} \min_c \quad & cS \left(\{\mathbf{w}_l^k\}_{l=0}^I, \mathbf{v}^k \right) + \frac{\lambda_c^k}{2} c^2 + \frac{\beta^k}{2} (c - c^k)^2 \\ \text{s.t.} \quad & c \in [0, C_k]. \end{aligned} \quad (31)$$

The optimization problem (31) can be solved in closed-form with a box constraint projection

$$c^{k+1} = \text{Proj}_{[0, C_k]} \left(\frac{\beta^k c^k - S \left(\{\mathbf{w}_l^k\}_{l=0}^I, \mathbf{v}^k \right)}{\lambda_c^k + \beta^k} \right). \quad (32)$$

Since the updating of \mathbf{y} and c involve simple operations, (26) can be solved very efficiently.

B. Obtaining the global optimal solution of (27)

Notice that $\{\mathbf{w}_l\}_{l=0}^I$ and \mathbf{v} are decoupled in both objective function and constraints of (27). Therefore, $\{\mathbf{w}_l^{k+1}\}_{l=0}^I$ and \mathbf{v}^{k+1} can be separately solved without losing the optimality.

Updating $\{\mathbf{w}_l\}_{l=0}^I$: Focusing on the terms related to $\{\mathbf{w}_l\}_{l=0}^I$ in (27), the maximization problem is given by

$$\begin{aligned} \min_{\{\mathbf{w}_l\}_{l=0}^I} & \sum_{l=0}^I \left\| \mathbf{w}_l - \left(\mathbf{w}_l^k + \frac{1}{\alpha^k} (\mathbf{y}^{k+1})^T \nabla_{\mathbf{w}_l} \psi \left(\{\mathbf{w}_l^k\}_{l=0}^I \right) \right. \right. \\ & \left. \left. + \frac{c^{k+1}}{\alpha^k} \nabla_{\mathbf{w}_l} S \left(\{\mathbf{w}_l^k\}_{l=0}^I, \mathbf{v}^k \right) \right) \right\|_2^2 \\ \text{s.t.} & \sum_{l=0}^I \|\mathbf{w}_l\|_2^2 \leq P_{BS}. \end{aligned} \quad (33)$$

Notice that the constraint of (33) is a sum power constraint, its closed-form solution is given by

$$\begin{aligned} \mathbf{w}_l^{k+1}(\chi) = & \frac{\alpha^k \mathbf{w}_l^k + (\mathbf{y}^{k+1})^T \nabla_{\mathbf{w}_l} \psi \left(\{\mathbf{w}_l^k\}_{l=0}^I \right)}{\alpha^k + 2\chi} \\ & + \frac{c^{k+1} \nabla_{\mathbf{w}_l} S \left(\{\mathbf{w}_l^k\}_{l=0}^I, \mathbf{v}^k \right)}{\alpha^k + 2\chi}, \end{aligned} \quad (34)$$

where $\chi = 0$ if $\sum_{l=0}^I \|\mathbf{w}_l^{k+1}(0)\|_2^2 \leq P_{BS}$. Otherwise, χ satisfies the equation $\sum_{l=0}^I \|\mathbf{w}_l^{k+1}(\chi)\|_2^2 = P_{BS}$, which can be found by the bisection method from the interval $[0, \sqrt{\frac{1}{4P_{BS}} \sum_{l=0}^I \|\alpha^k \mathbf{w}_l^k(0)\|_2^2}]$.

Updating \mathbf{v} : From (21), the optimization problem w.r.t. \mathbf{v} is given by

$$\begin{aligned} \min_{\mathbf{v}} & \left\| \mathbf{v} - (\mathbf{v}^k + c^{k+1} \nabla_{\mathbf{v}} S(\{\mathbf{w}_l^k\}_{l=0}^I, \mathbf{v}^k) / \alpha^k) \right\|_2^2 \\ \text{s.t.} & \mathbf{v} \in \Omega_{\mathbf{v}}. \end{aligned} \quad (35)$$

This is a simple projection problem and the optimal solution is

$$\mathbf{v}^{k+1} = \text{Proj}_{\Omega_{\mathbf{v}}}(\mathbf{v}^k + c^{k+1} \nabla_{\mathbf{v}} S(\{\mathbf{w}_l^k\}_{l=0}^I, \mathbf{v}^k) / \alpha^k). \quad (36)$$

Notice that (34) and (36) only contain simple one dimensional bisection search and projection update, thus solving (27) is very efficient.

C. Computation of gradients in various ISAC scenarios

Notice that computation of various gradients only occurs when solving (27). As an example, we compute the gradient $\nabla_{\mathbf{w}_l} \psi \left(\{\mathbf{w}_l^k\}_{l=0}^I \right)$ when $\psi_i(\cdot)$ is the secrecy rate $\{\mathcal{R}_i(\{\mathbf{w}_l\}_{l=0}^I) - D_i(\{\mathbf{w}_l\}_{l=0}^I)\}_{\forall i}$:

$$\begin{aligned} \nabla_{\mathbf{w}_l} \psi \left(\{\mathbf{w}_l\}_{l=0}^I \right) & = \left[\nabla_{\mathbf{w}_l} \mathcal{R}_1 \left(\{\mathbf{w}_l\}_{l=0}^I \right) - \nabla_{\mathbf{w}_l} D_1 \left(\{\mathbf{w}_l\}_{l=0}^I \right), \dots, \right. \\ & \left. \nabla_{\mathbf{w}_l} \mathcal{R}_I \left(\{\mathbf{w}_l\}_{l=0}^I \right) - \nabla_{\mathbf{w}_l} D_I \left(\{\mathbf{w}_l\}_{l=0}^I \right) \right], \end{aligned} \quad (37)$$

where $\nabla_{\mathbf{w}_l} \mathcal{R}_i(\{\mathbf{w}_l\}_{l=0}^I)$ and $\nabla_{\mathbf{w}_l} D_i(\{\mathbf{w}_l\}_{l=0}^I)$ are respectively given in (38) (shown at the top of this page), and $\tau_{i,t} = \|\mathbf{w}_i\|_2^2 + (2^{D_i(\{\mathbf{w}_l\}_{l=0}^I)} - 1) \|\mathbf{w}_t\|_2^2$. If there is no eavesdropper, we can just set $D_i(\{\mathbf{w}_l\}_{l=0}^I) \equiv 0$.

On the other hand, we need $\{\nabla_{\mathbf{w}_l} S(\{\mathbf{w}_l\}_{l=0}^I, \mathbf{v})\}_{\forall l}$ and $\nabla_{\mathbf{v}} S(\{\mathbf{w}_l\}_{l=0}^I, \mathbf{v})$ in (34) and (36), respectively. Below,

we list the gradients of three sensing performance metrics mentioned in Section III.

1) Sensing SINR: In this case, $\mathbf{v} = \mathbf{u}$, and $S(\{\mathbf{w}_l\}_{l=0}^I, \mathbf{v})$ is given by the left hand side of (13a). Correspondingly, the gradients of $S(\{\mathbf{w}_l\}_{l=0}^I, \mathbf{v})$ are given as

$$\begin{aligned} \nabla_{\mathbf{w}_l} S \left(\{\mathbf{w}_l\}_{l=0}^I, \mathbf{v} \right) & = 2\mathbf{A}_0^H \bar{\mathbf{v}} \mathbf{v}^T \mathbf{A}_0 \mathbf{w}_l \\ & \quad - 2\Gamma \sum_{m=1}^M \mathbf{A}_m^H \bar{\mathbf{v}} \mathbf{v}^T \mathbf{A}_m \mathbf{w}_l. \end{aligned} \quad (39a)$$

$$\begin{aligned} \nabla_{\mathbf{u}} S \left(\{\mathbf{w}_l\}_{l=0}^I, \mathbf{v} \right) & = 2 \sum_{l=0}^I \bar{\mathbf{A}}_0 \bar{\mathbf{w}}_l \mathbf{w}_l^T \mathbf{A}_0^T \mathbf{v} \\ & \quad - 2\Gamma \sum_{l=0}^I \sum_{m=1}^M \bar{\mathbf{A}}_m \bar{\mathbf{w}}_l \mathbf{w}_l^T \mathbf{A}_m^T \mathbf{v}. \end{aligned} \quad (39b)$$

Then, the update of $\{\mathbf{w}_l^{k+1}\}_{l=0}^I$ can be obtained by putting (39a) back to (34). For the update of \mathbf{v} , since $\Omega_{\mathbf{v}}$ is a normalization constraint, the optimal solution \mathbf{v}^{k+1} is given by $\mathbf{v}^{k+1} = \frac{\alpha^k \mathbf{v}^k + c^{k+1} \nabla_{\mathbf{v}} S(\{\mathbf{w}_l^k\}_{l=0}^I, \mathbf{v}^k)}{\|\alpha^k \mathbf{v}^k + c^{k+1} \nabla_{\mathbf{v}} S(\{\mathbf{w}_l^k\}_{l=0}^I, \mathbf{v}^k)\|_2}$.

2) Beampattern matching: In this case, $\Omega_{\mathbf{v}} = \emptyset$, and $S(\{\mathbf{w}_l\}_{l=0}^I) = \gamma - \text{MSE}(\{\mathbf{w}_l\}_{l=0}^I)$, where $\text{MSE}(\{\mathbf{w}_l\}_{l=0}^I)$ is given by (18). Then, the gradient of $S(\{\mathbf{w}_l\}_{l=0}^I)$ is given as

$$\begin{aligned} \nabla_{\mathbf{w}_l} S \left(\{\mathbf{w}_l\}_{l=0}^I \right) & = \frac{4}{T} \sum_{t=1}^T \\ & \left[P_d(\theta_t) - \mathbf{a}^H(\theta_t) \left(\sum_{i=0}^I \mathbf{w}_i \mathbf{w}_i^H \right) \mathbf{a}(\theta_t) \right] \mathbf{a}(\theta_t) \mathbf{a}^H(\theta_t) \mathbf{w}_l. \end{aligned} \quad (40)$$

The update of $\{\mathbf{w}_l^{k+1}\}_{l=0}^I$ is obtained by putting (40) to (34). Since \mathbf{v} does not appear in the sensing metric, there is no optimization step for \mathbf{v} .

3) Detection probability: In this case, $\Omega_{\mathbf{v}} = \emptyset$, and $S(\{\mathbf{w}_l\}_{l=0}^I)$ is given by the left hand side of (22), which gives the gradient of $S(\{\mathbf{w}_l\}_{l=0}^I)$ as

$$\nabla_{\mathbf{w}_l} S \left(\{\mathbf{w}_l\}_{l=0}^I \right) = 2\mathbf{A}_0 \mathbf{w}_l. \quad (41)$$

Similar to the above two cases, the update of $\{\mathbf{w}_l^{k+1}\}_{l=0}^I$ is obtained by putting (41) to (34). Similar to beampattern matching case, there is no \mathbf{v} in the sensing metric, the corresponding optimization step can be skipped.

Notice that the proposed algorithm can handle sensing metrics beyond the above cases. When a new sensing metric is employed, the only change involved is the gradients $\nabla_{\mathbf{w}_l} S(\{\mathbf{w}_l^k\}_{l=0}^I, \mathbf{v}^k)$ and $\nabla_{\mathbf{v}} S(\{\mathbf{w}_l^k\}_{l=0}^I, \mathbf{v}^k)$, while other parts of the algorithm remain the same. For example, if the sensing metric is the mutual information (MI) [76], we have $S(\{\mathbf{w}_l\}_{l=0}^I) = \log_2 \left(1 + \frac{1}{\sigma_{BS}^2} \sum_{l=0}^I \mathbf{w}_l^H \left(\sum_{m=0}^M \mathbf{A}_m^H \mathbf{A}_m \right) \mathbf{w}_l \right) - \delta$, where δ is the minimal MI needed for sensing, and there is no \mathbf{v} . To connect with the proposed framework, we only need to compute the gradient of $S(\{\mathbf{w}_l\}_{l=0}^I)$ and replace

$$\nabla_{\mathbf{w}_l} \mathcal{R}_i(\{\mathbf{w}_l\}_{l=0}^I) = \begin{cases} \frac{2\bar{\mathbf{h}}_i \mathbf{h}_i^T \mathbf{w}_l}{\left(\sum_{t=0}^I |\mathbf{h}_i^T \mathbf{w}_t|^2 + \sigma_i^2\right) \ln 2} - \frac{2\bar{\mathbf{h}}_i \mathbf{h}_i^T \mathbf{w}_l}{\left(\sum_{t=0, t \neq i}^I |\mathbf{h}_i^T \mathbf{w}_t|^2 + \sigma_i^2\right) \ln 2}, & l \neq i, \\ 2\bar{\mathbf{h}}_i \mathbf{h}_i^T \mathbf{w}_l / \left[\left(\sum_{t=0}^I |\mathbf{h}_i^T \mathbf{w}_t|^2 + \sigma_i^2\right) \ln 2 \right], & l = i. \end{cases} \quad (38a)$$

$$\nabla_{\mathbf{w}_l} D_i(\{\mathbf{w}_l\}_{l=0}^I) = \begin{cases} \frac{\left(1 - 2^{D_i(\{\mathbf{w}_l\}_{l=0}^I)}\right) 2\mathbf{w}_l}{2^{D_i(\{\mathbf{w}_l\}_{l=0}^I)} \tau_{i,l} \left[\frac{\ln 2}{\max_j \{\rho_j^2 / \varsigma_j^2\} \|\mathbf{w}_i\|_2^2 + \sum_{t=0, t \neq i}^I \frac{\|\mathbf{w}_t\|_2^2 \ln 2}{\tau_{i,t}}} \right]}, & l \neq i, \\ \left(2^{D_i(\{\mathbf{w}_l\}_{l=0}^I)} - 1\right) 2\mathbf{w}_i / \left[\|\mathbf{w}_i\|_2^2 2^{D_i(\{\mathbf{w}_l\}_{l=0}^I)} \ln 2 \right], & l = i. \end{cases} \quad (38b)$$

TABLE I
Computational complexity of Algorithm 1

	Computational complexity
Algorithm without gradient update of $S(\{\mathbf{w}_l\}_{l=0}^I, \mathbf{v})$	$\mathcal{O}(KI^2N + KI^2 \log(\xi_D^{-1}) + KI \log(\xi_{\mathbf{y}}^{-1}) + KNI \log(\xi_{\mathbf{w}}^{-1}))$
Gradient update under sensing SINR	$K \cdot \mathcal{O}(MNI) + K \cdot \mathcal{O}_{\mathbf{v}}$
Gradient update under beampattern matching	$K \cdot \mathcal{O}(TNI)$
Gradient update under detection probability	$K \cdot \mathcal{O}(NI)$

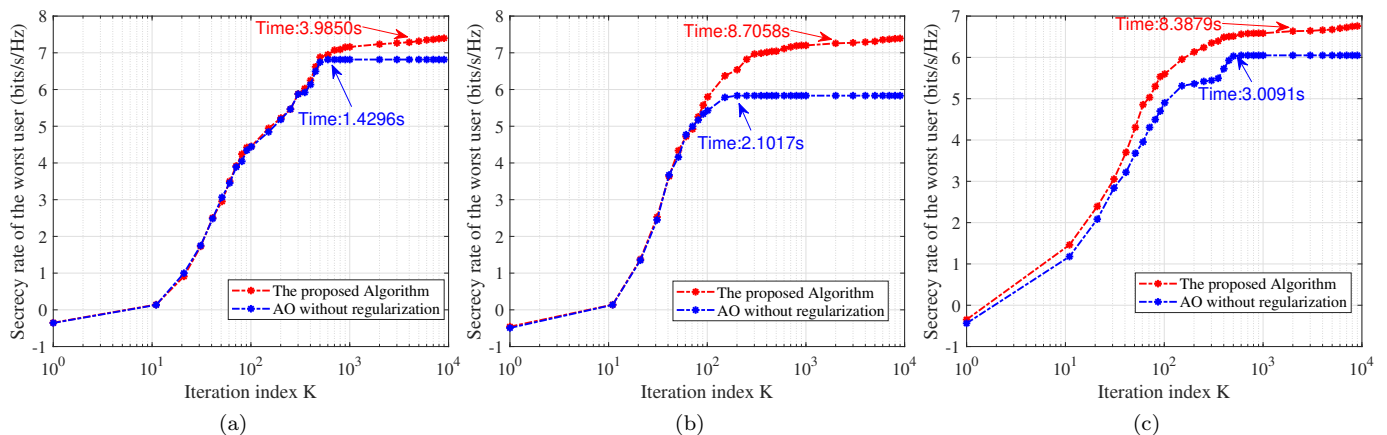


Fig. 2. Worst user secrecy rate performance with $I = 5$, $J = 8$, $N = 20$, $M = 5$, $P_{BS} = 20$ dBm. (a) $\Gamma = 10$ dB under sensing SINR constraint, (b) $\gamma = 0.1$ under beampattern matching constraint, (c) $P_{FA} = 0.1$ and $\phi = 0.9$ under detection probability constraint

$\nabla_{\mathbf{w}_l} S(\{\mathbf{w}_l\}_{l=0}^I, \mathbf{v}^k)$ in (34) with the gradient of the MI metric. This advantage makes the proposed algorithm widely applicable to different ISAC scenarios.

Overall, the complexity of Algorithm 1 is summarized in Table I, where ξ_D , $\xi_{\mathbf{y}}$ and $\xi_{\mathbf{w}}$ are the accuracy of the bisection search in redundancy rate $\{D_i\}_{i=1}^I$, auxiliary vector \mathbf{y} and beamformers $\{\mathbf{w}_l\}_{l=0}^I$, respectively. For the complexity of calculating the gradient of $S(\{\mathbf{w}_l\}_{l=0}^I, \mathbf{v})$ with respect to $\{\mathbf{w}_l\}_{l=0}^I$ in a single iteration, it is $\mathcal{O}(MNI)$, $\mathcal{O}(TNI)$ and $\mathcal{O}(NI)$ for the sensing SINR, beampattern matching and detection probability, respectively. $\mathcal{O}_{\mathbf{v}}$ is the complexity of updating \mathbf{v} in a single iteration, which involves calculating the gradient of $S(\{\mathbf{w}_l\}_{l=0}^I, \mathbf{v})$ with respect to \mathbf{v} and the projection operation in (34). As \mathbf{v} only appears in the sensing SINR case, $\mathcal{O}_{\mathbf{v}} = \mathcal{O}(MNI)$.

VI. Simulation Results and Discussions

In this section, we evaluate the performance of the proposed algorithm through simulations, with each point in the figures obtained via averaging over 100 simulation trials. In the simulations, the position of the legitimate users, eavesdroppers, scatterings and BS are randomly distributed in a circular area with a radius of 100m. The carrier frequency is 3.5GHz, the bandwidth is set to 10 MHz and the noise power spectral density for legitimate users, eavesdroppers and BS are $\sigma_i^2 = \varsigma_j^2 = \sigma_{BS}^2 = -96$ dBm/Hz [75]. The target secrecy outage probability level $\eta_i = 0.1$. For the proposed algorithm, the regularization parameters at the k^{th} iteration are $\lambda_c^k = \lambda_{\mathbf{y}}^k = k^{-\frac{1}{4}}$, $\beta^k = k^{-3}$, $\alpha^k = k^{\frac{1}{3}}$ and $C^k = 10 + \ln k$, which are set according to Proposition 2. The variance of the statistical CSI of eavesdroppers $\{\rho_j\}_{j \in \mathcal{V}_j}$ is set according to [75], which follows the signal propagation model. The

round-trip channel coefficients $\{\beta_m\}_{\forall m}$ of the scatterings are set as β_m (dB) = $20 + 20\log_{10}(d_m)$ [77], where d_m is the Euclidean distances between the BS and the m^{th} scattering. The number of sampling angles $T = 181$ in beam pattern matching case are uniformly distributed over the range from -90° to 90° [58], and the desired beam pattern $P_d(\theta_i)$ follows that from [14, eq. 11]. The channels $\{\mathbf{h}_i\}_{\forall i}$ of the legitimate users are modeled as Rician fading, which contain both the line-of-sight (LoS) and non-LoS (NLoS) components [78], and is given by

$$\mathbf{h}_i = \sqrt{L_0(d_{\mathbf{h}_i}/d_0)^{-\alpha_h}} / (\kappa_h + 1) (\sqrt{\kappa_h} \mathbf{h}_i^{\text{LoS}} + \mathbf{h}_i^{\text{NLoS}}),$$

with each parameter explained below.

- 1) $L_0(d_{\mathbf{h}_{k,i}}/d_0)^{-\alpha_h}$ is the distance dependent pathloss from the BS to the i^{th} legitimate user, where $L_0 = -30\text{dB}$ denotes the pathloss at the reference distance $d_0 = 1\text{m}$. The parameter $d_{\mathbf{h}_i}$ is the distance between the BS and the i^{th} legitimate user, $\alpha_h = 2$ denotes the pathloss exponent for the BS-user link, and $\kappa_h = 5$ is the Rician factor of the BS-user link.
- 2) The LoS component $\mathbf{h}_i^{\text{LoS}}$ is modeled as the response vector of a uniform linear array. Hence the n^{th} element $[\mathbf{h}_i^{\text{LoS}}]_n = e^{j2\pi(n-1)\zeta \sin(\omega)}$, where ω denotes the angle-of-arrival (AoA) or angle-of-departure (AoD) of the array, which is uniformly distributed in $[0, 2\pi)$ and $\zeta = 1/2$. On the other hand, $\mathbf{h}_i^{\text{NLoS}}$ denotes the NLoS channel component with each element obeying the normalized complex Gaussian distribution.

First, we show the convergence of the proposed method for worst secrecy rate maximization under three different sensing criteria in Fig. 2. Here, the times in these figures are counted at the iterations where the arrows point to. Furthermore, to demonstrate the importance of regularizing the AO minimization subproblem (24), we also include the simulation of directly executing (24) without regularization. As can be seen from Fig. 2, the proposed AO iteration converges fast, with the secrecy rate at $K = 1000$ iterations reaches at least 95% of that at $K = 10000$ iterations. Furthermore, the performance degradation resulting from not regularizing (24) under the criteria of sensing SINR, beam pattern matching and detection probability are 11.51%, 29.73% and 15.47%, respectively. This degradation is due to possibly unbounded solution of (24), which hinders the subsequent iterations and leads to premature termination of the process. Notice that the usual termination condition, such as the improvement of the objective function between two adjacent iterations being less than a certain tolerance (e.g., 10^{-4}), does not apply to the proposed algorithm since it involves non-monotonic iterations. Actually, proper selection of the number of iterations is still an open problem in non-monotonic iterative algorithms [67], [68], which involves the trade-off between the computational time and the performance. In the subsequent simulations, we take results at $K = 1000$ and $K = 10000$ iterations to demonstrate the performance of the proposed algorithm.

Next, we compare the worst user secrecy rate performance of the proposed algorithm with other optimization

methods. The compared approaches are labeled in the form of $A+B$, where A represents the way of handling the inner minimization in (8a) while B denotes the method for handling the sensing constraint and SOP constraint after applying the Lemma 1. In particular, for handling the inner minimization, we consider either penalty reformulation or auxiliary variable substitution. In penalty reformulation, it uses the log-sum-exp function with an additional penalty weight to approximate the inner minimization problem [47]. On the other hand, in auxiliary variable substitution, the inner minimization problem is replaced with an auxiliary variable, and moved as a constraint [79]. For handling the resultant transformed problem, we consider SDR, projected gradient ascent or SCA. However, notice that the projected gradient ascent cannot be applied to the transformed problem obtained by auxiliary variable substitution since the transformed objective function does not depend on the beamformers $\{\mathbf{w}_i\}_{i=0}^I$ and the vector \mathbf{v} in the sensing constraint anymore, and thus its derivative with respect to these variables are all zeros. This results in a total of 5 methods being compared. The running times of each algorithm in Figs. 3 - 4 are averaged over all simulated settings in each figure.

As can be seen in Figs. 3(a) and 4(a), which shows the secrecy rate of the worst user under sensing SINR constraint, the proposed algorithm achieves the best secrecy rate. This is due to the following two reasons. Firstly, through the introduced dual variable c , the sensing performance constraint is put as part of the objective function. This means that at early stages of iteration, the sensing performance constraint can be violated, which enlarges the feasible set and increases the flexibility of finding a better iteration trajectory. As the iteration goes, the dual variable c would gradually pull the iteration points to satisfy the sensing performance constraint. In this way, the sensing performance constraint is enforced by the proposed algorithm as a soft margin constraint with the margin increasingly tightened. This is in great contrast to other algorithms that treat the sensing performance constraint as hard constraint in all iterations. Secondly, since we alternatively optimize the max layer and min layer, the iteration process is non-monotonic. This enables the proposed algorithm to cross the valley of the bumpy surface to find a better solution. However, other algorithms are monotonic and they cannot go over a valley to find a solution with higher worst case secrecy rate.

Besides the advantage of obtaining the best secrecy rate, the proposed algorithm also enjoys one of the lowest running times. Although the auxiliary variable substitution combined with SCA costs the least time, its secrecy rate is the worst and the solution is practically useless. In general, applying SCA and SDR rely on conventional convex tools such as CVX for solving the resulting problems, which lead to high computational complexity. For the penalty reformulation combined with projected gradient ascent method, while it uses the gradient information and thus mitigate the computation burden, it still requires explicit handling of the sensing performance constraint $S(\mathbf{w}, \mathbf{u}) \geq$

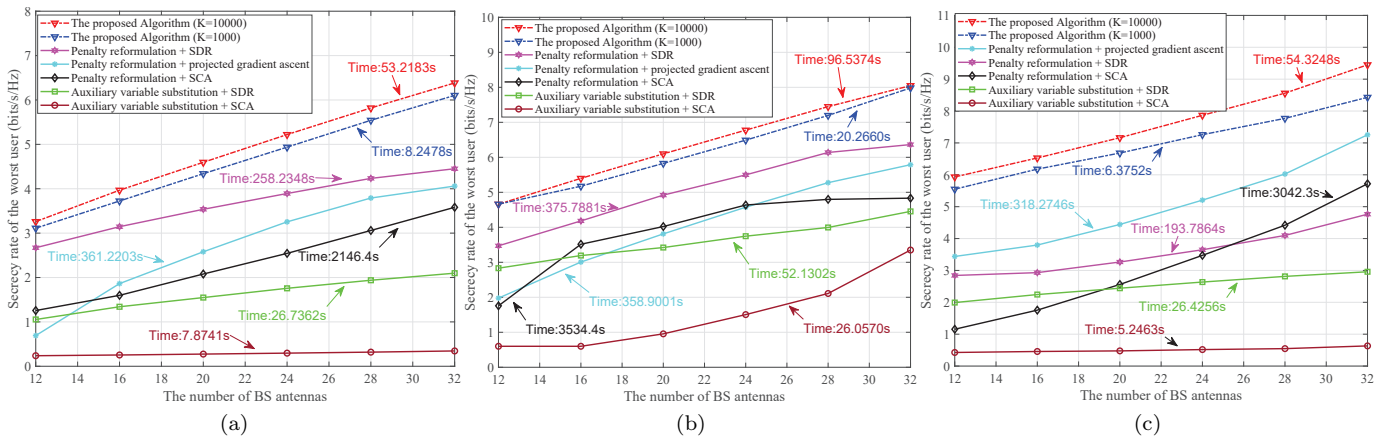


Fig. 3. Worst user secrecy rate versus number of BS antennas under three different sensing metrics. Simulation settings: (a) $I = 7$, $J = 9$, $M = 6$, $P_{BS} = 20\text{dBm}$ and $\Gamma = 10\text{dB}$ for sensing SINR constraint; (b) $I = 5$, $J = 7$, $M = 4$, $P_{BS} = 20\text{dBm}$ and $\gamma = 0.1$ for beampattern matching constraint; (c) $I = 6$, $N = 28$, $M = 7$, $P_{BS} = 15\text{dBm}$, $P_{FA} = 0.1$ and $\phi = 0.85$ for detection probability constraint.

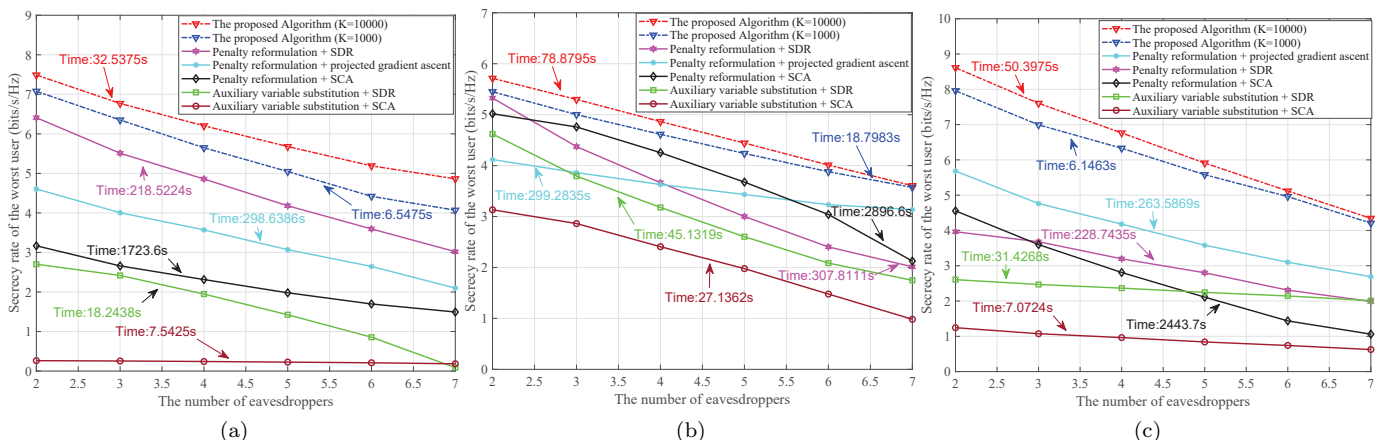


Fig. 4. Worst user secrecy rate versus number of eavesdroppers under three different sensing metrics. Simulation settings: (a) $I = 7$, $N = 24$, $M = 6$, $P_{BS} = 15\text{dBm}$ and $\Gamma = 10\text{dB}$ for sensing SINR constraint; (b) $I = 5$, $N = 24$, $M = 4$, $P_{BS} = 10\text{dBm}$ and $\gamma = 0.1$ for beampattern matching constraint; (c) $I = 6$, $J = 4$, $M = 7$, $P_{BS} = 20\text{dBm}$, $P_{FA} = 0.1$ and $\phi = 0.9$ for detection probability constraint.

0 in every iteration, which does not have closed-form solutions or simple one-dimensional bisection solutions as in the proposed algorithm. In contrast, the proposed algorithm only consists of computing gradients and simple calculations. As a result, the proposed algorithm costs significantly less time than the other methods.

Under the beampattern matching sensing criterion, the worst secrecy rates due to various methods are shown in Figs. 3(b) and 4(b), which again shows the proposed algorithm is having the best performance. Notice that the beampattern matching sensing constraint is more complex than the SINR sensing constraint since it is a function containing the fourth power of beamformers $\{\mathbf{w}_l\}_{l=0}^T$ and its summation depends on the number of sampling angles T . This would increase the load of computing the gradients compared to the SINR constraint. In the compared methods, auxiliary variables are needed to replace the whole absolute value function (18), which would generate more auxiliary constraints and greatly slows down the compared methods. Although all the methods takes more time in

beampattern matching constraint compared to the case of SINR constraint, calculating gradients is relatively more efficient than convexifying the complex sensing constraint. This leads to the proposed algorithm being one of the fastest algorithms among the compared methods.

The worst user secrecy rate performance of various algorithms under detection probability sensing constraint are shown in Figs. 3(c) and 4(c). Since the detection probability constraint is a summation of quadratic terms w.r.t. beamformers $\{\mathbf{w}_l\}_{l=0}^T$, the convex surrogate function in SCA can be chosen as the first-order Taylor expansion of these quadratic terms. Alternatively, we can transform these quadratic terms into matrix variables and then relax the problem to a semidefinite programming (SDP). Similar to the sensing SINR constraint and beampattern matching constraint cases, the proposed algorithm achieves the best secrecy rate performance with the one of the shortest execution times.

Furthermore, the realized sensing performance under different thresholds of the sensing constraints is shown in

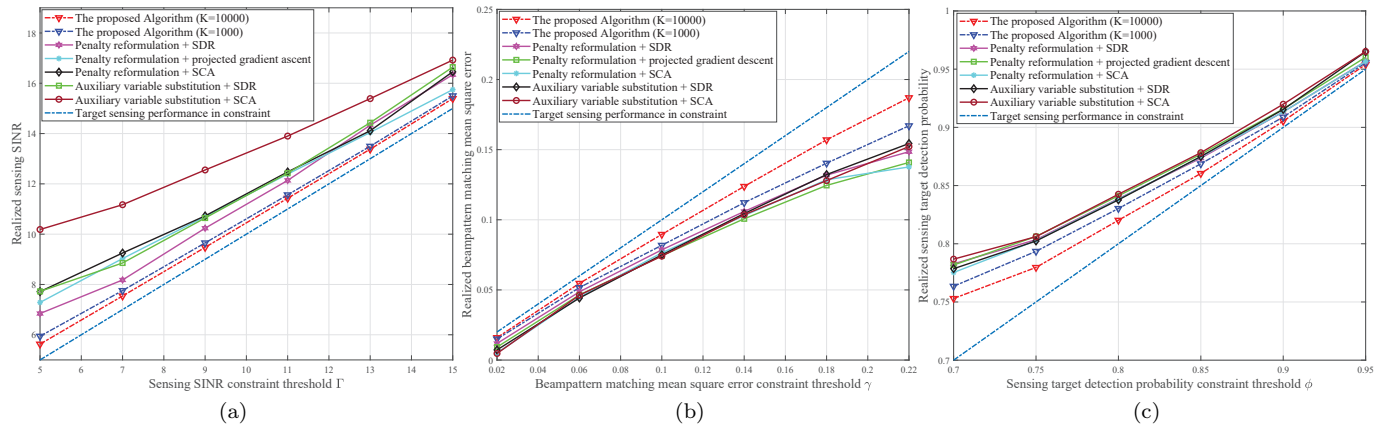


Fig. 5. Realized sensing performance under different sensing constraint thresholds (a) $N = 20$, $I = 6$, $J = 7$, $M = 5$, $P_{BS} = 20\text{dBm}$ with sensing SINR metric, (b) $N = 16$, $I = 5$, $J = 4$, $M = 6$, $P_{BS} = 20\text{dBm}$ with beampattern matching metric, (c) $N = 12$, $I = 6$, $J = 5$, $M = 4$, $P_{BS} = 20\text{dBm}$, $P_{FA} = 0.1$ with detection probability metric

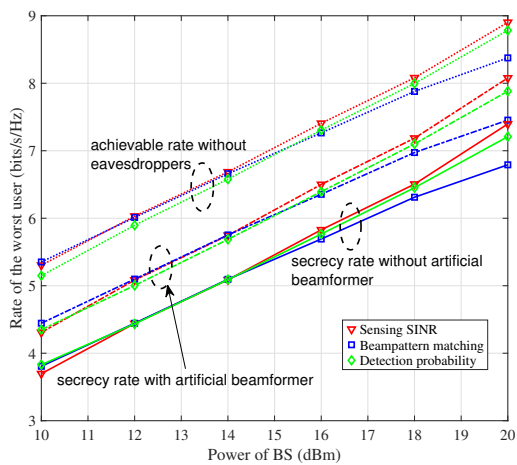


Fig. 6. Worst user rate performance under three sensing metrics with $N = 24$, $I = 7$, $J = 5$, $M = 4$. $\Gamma = 10\text{dB}$ under sensing SINR constraint, $\gamma = 0.1$ under beampattern matching constraint, $P_{FA} = 0.1$ and $\phi = 0.9$ under detection probability constraint.

Fig. 5. From the figure, it can be seen that the proposed algorithm achieves realized sensing performance closest to the target specified in the sensing constraints (represented by the light blue line). Therefore, the proposed algorithm does not spend excessive resource to over-satisfy the sensing constraint, which leaves more resource for optimizing the secrecy rate. This explains the best secrecy rate achieved by the proposed algorithm compared to other existing methods in Figs. 3 and 4. The trade-off between sensing and secure communication performance is further shown in Fig. S1 in the supplementary material.

Next, we show the impact of the eavesdroppers and the benefit of artificial beamformer \mathbf{w}_0 in Fig. 6. As expected, eavesdroppers would degrade the performance. Without artificial beamformer, the degradation could reach 33% for all three considered sensing constraints. This shows that eavesdroppers cannot be neglected in ISAC. However, adopting artificial beamformer, which on the surface would

take away some power resource from legitimate users, ends up improving the secrecy rate and leads to only 17% degradation compared to no eavesdropper case. The artificial beamformer serves two purposes here: it provides a beam for sensing the target to facilitate the satisfaction of the sensing constraint and at the same time acts as artificial noise to counteract the eavesdroppers.

Finally, to show the versatility of the proposed general formulation and solution framework, Fig. 7 illustrates the sum secrecy rate performance under three different sensing metrics with various sensing constraint thresholds. Due to the same advantages mentioned in worst user secrecy rate maximization, the proposed algorithm also enjoys better performance and lower running time compared to other algorithms in sum rate maximization.

VII. Conclusions

This paper presented a unified optimization framework for maximizing the secrecy rate under various sensing constraints in secure ISAC systems. It was revealed that the probabilistic outage constraint can be handled precisely so that the limited resource could be better utilized for secrecy rate optimization. By transforming sensing constraints into the objective function and introducing a penalty variable, the proposed framework efficiently accommodates various sensing metrics, including (but not limited) to sensing SINR, beampattern matching, and detection probability. The resultant optimization problem was solved with AO algorithm enhanced with regularization, and the solution was theoretically proved to converge to a stationary point. Simulation results validated the effectiveness and computational efficiency of the framework in optimizing the secrecy rates across various sensing criteria, outperforming other state-of-the-art methods. This unified framework not only streamlines algorithmic development for future research in secure ISAC systems but also facilitates straightforward comparisons across different scenarios.

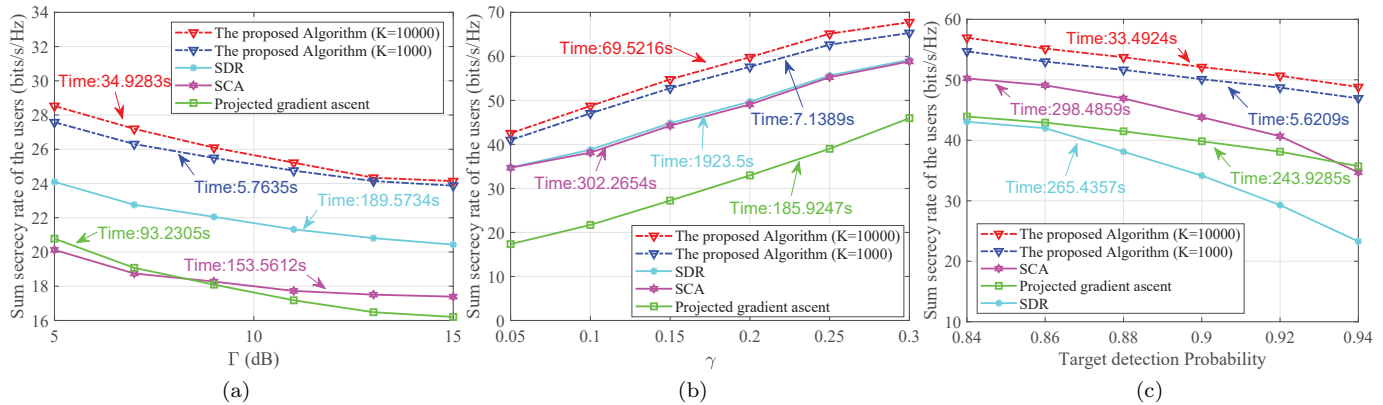


Fig. 7. Sum secrecy rate versus constraint thresholds under three different sensing metric. Simulation settings: (a) $N = 16$, $I = 4$, $J = 5$, $M = 3$, $P_{BS} = 10\text{dBm}$ for sensing SINR constraint; (b) $N = 24$, $I = 7$, $J = 5$, $M = 6$, $P_{BS} = 15\text{dBm}$ for beam pattern matching constraint; (c) $N = 24$, $I = 6$, $J = 7$, $M = 5$, $P_{BS} = 15\text{dBm}$ and $P_{FA} = 0.1$ for detection probability constraint.

References

- [1] B. Tan, Q. Chen, K. Chetty, K. Woodbridge, W. Li, and R. Piechocki, "Exploiting wifi channel state information for residential healthcare informatics," *IEEE Commun. Mag.*, vol. 56, no. 5, pp. 130–137, May 2018.
- [2] D. W. Bliss, "Cooperative radar and communications signaling: The estimation and information theory odd couple," *Proc.-IEEE Natl. Radar Conf.*, pp. 50–55, May 2014.
- [3] S. Lu, F. Liu, Y. Li, K. Zhang, H. Huang, J. Zou, X. Li, Y. Dong, F. Dong, J. Zhu, Y. Xiong, W. Yuan, Y. Cui, and L. Hanzo, "Integrated sensing and communications: Recent advances and ten open challenges," *IEEE Internet Things J.*, vol. 11, no. 11, pp. 19094–19120, Feb 2024.
- [4] Z. Han, Y. Zhou, Y. Zhang, T.-X. Zheng, L. Liu, and J. Shi, "Joint jammer selection and power optimization in covert communications against a warden with uncertain locations," *Digit. Commun. Netw.*, vol. 11, no. 4, pp. 1114–1124, Aug 2025.
- [5] N. Su, F. Liu, and C. Masouros, "Secure integrated sensing and communication systems with the assistance of sensing functionality," *Proc. - EUSIPCO 2023*, pp. 690–694, Nov 2023.
- [6] W.-Y. Keung, H.-T. Wai, and W.-K. Ma, "Secure integrated sensing and communication downlink beamforming: A semidefinite relaxation approach with tightness guaranteed," *Proc. - ICASSP 2023*, pp. 1–5, Aug 2023.
- [7] K. Hou and S. Zhang, "Optimal beamforming for secure integrated sensing and communication exploiting target location distribution," *IEEE J. Sel. Areas Commun.*, vol. 42, no. 11, pp. 3125–3139, Aug 2024.
- [8] Y. Liu, X. Liu, Z. Liu, Y. Yu, M. Jia, Z. Na, and T. S. Durrani, "Secure rate maximization for isac-uav assisted communication amidst multiple eavesdroppers," *IEEE Trans. Veh. Technol.*, vol. 73, no. 10, pp. 15843–15847, Oct 2024.
- [9] Z. Yang, D. Li, N. Zhao, Z. Wu, Y. Li, and D. Niyato, "Secure precoding optimization for noma-aided integrated sensing and communication," *IEEE Trans. Commun.*, vol. 70, no. 12, pp. 8370–8382, Oct 2022.
- [10] X. Zhao, W. Deng, M. Li, and M.-J. Zhao, "Robust beamforming design for integrated sensing and covert communication systems," *IEEE Wireless Commun. Lett.*, vol. 13, no. 9, pp. 2566–2570, Jul 2024.
- [11] H. Jia, L. Ma, and D. Qin, "Robust beamforming design for covert integrated sensing and communication in the presence of multiple wardens," *IEEE Trans. Veh. Technol.*, vol. 73, no. 11, pp. 17135–17150, Jul 2024.
- [12] Y. Zhang, W. Ni, J. Wang, W. Tang, M. Jia, Y. C. Eldar, and D. Niyato, "Robust transceiver design for covert integrated sensing and communications with imperfect csi," *IEEE Transactions on Communications*, vol. 73, no. 9, pp. 8016–8031, Apr 2025.
- [13] N. Su, F. Liu, and C. Masouros, "Secure radar-communication systems with malicious targets: Integrating radar, communications and jamming functionalities," *IEEE Trans. Wireless Commun.*, vol. 20, no. 1, pp. 83–95, Sep 2021.
- [14] P. Liu, Z. Fei, X. Wang, B. Li, Y. Huang, and Z. Zhang, "Outage constrained robust secure beamforming in integrated sensing and communication systems," *IEEE Wireless Commun.*, vol. 11, no. 11, pp. 2260–2264, Aug 2022.
- [15] Y. Liu, M. Jin, Q. Guo, and J. Yao, "Secure beamforming for noma-isac with system imperfections," *IEEE Commun. Lett.*, vol. 28, no. 7, pp. 1559–1563, May 2024.
- [16] Z. Wang, X. Lei, P. T. Mathiopoulos, and G. Wang, "Transmit power optimization of cooperative noma-aided secure isac systems with swipt," *IEEE Trans. Veh. Technol.*, vol. 74, no. 8, pp. 13207–13212, Mar 2025.
- [17] Y. Xiu, W. Lyu, P. L. Yeoh, Y. Ai, and N. Wei, "Secure enhancement for ris-aided uav with isac: Robust design and resource allocation," *IEEE Trans. Veh. Technol.*, pp. 1–16, Oct 2025.
- [18] C. Zhang, S. Qu, L. Zhao, Z. Wei, Q. Shi, and Y. Liu, "Robust secure beamforming design for downlink ris-isac systems enhanced by rsma," *IEEE Wireless Commun. Lett.*, vol. 14, no. 5, pp. 1271–1275, Dec 2025.
- [19] M. Hua, Q. Wu, W. Chen, O. A. Dobre, and A. L. Swindlehurst, "Secure intelligent reflecting surface-aided integrated sensing and communication," *IEEE Trans. Wireless Commun.*, vol. 23, no. 1, pp. 575–591, Jun 2024.
- [20] W. Wang, K. C. Teh, and K. H. Li, "Secrecy throughput maximization for miso multi-eavesdropper wiretap channels," *IEEE Trans. Inf. Forensics Secur.*, vol. 12, no. 3, pp. 505–515, Oct 2017.
- [21] X. Zhang, M. R. McKay, X. Zhou, and R. W. Heath, "Artificial-noise-aided secure multi-antenna transmission with limited feedback," *IEEE Trans. Wireless Commun.*, vol. 14, no. 5, pp. 2742–2754, Jan 2015.
- [22] Q. Xiong, Y. Gong, Y.-C. Liang, and K. H. Li, "Achieving secrecy of miso fading wiretap channels via jamming and precoding with imperfect channel state information," *IEEE Wireless Commun. Lett.*, vol. 3, no. 4, pp. 357–360, Apr 2014.
- [23] H.-M. Wang, T. Zheng, and X.-G. Xia, "Secure miso wiretap channels with multiantenna passive eavesdropper: Artificial noise vs. artificial fast fading," *IEEE Trans. Wireless Commun.*, vol. 14, no. 1, pp. 94–106, Jun 2015.
- [24] H. Zhao, F. Wu, W. Xia, Y. Zhang, Y. Ni, and H. Zhu, "Joint beamforming design for ris-aided secure integrated sensing and communication systems," *IEEE Commun. Lett.*, vol. 27, no. 11, pp. 2943–2947, Sep 2023.
- [25] W. Yang, X. Liu, and Z. Liu, "Joint trajectory and resource allocation optimization for mobile vehicles in uav assisted secure isac system," *Proc. - ICCT 2024*, pp. 321–325, Oct 2024.
- [26] A. A. Salem, S. Abdallah, M. Saad, K. Alnajjar, and M. A. Albreem, "Robust secure isac: How rsma and active ris manage eavesdropper's spatial uncertainty," *IEEE Trans. Veh. Technol.*, pp. 1–16, Sep 2025.

- [27] X. Chen, X. Cao, L. Xie, and Y. He, "DRL-based joint trajectory planning and beamforming optimization in aerial ris-assisted isac system," *Proc - IEEE iWRFAT*, pp. 510–515, Jul 2024.
- [28] X. Li, Z. Wu, Y. Cai, S. Hu, Y. Liao, and W. Yuan, "Win-win of communication and sensing security for mc-noma isac systems," *IEEE J. Sel. Areas Commun.*, vol. 43, no. 9, pp. 3214 – 3230, May 2025.
- [29] Z. Liu, X. Liu, Y. Liu, V. C. M. Leung, and T. S. Durrani, "Uav assisted integrated sensing and communications for internet of things: 3d trajectory optimization and resource allocation," *IEEE Trans. Wireless Commun.*, vol. 23, no. 8, pp. 8654–8667, Jan 2024.
- [30] R. Yang and H. Du, "Joint precoding and artificial noise design for secure transmission in isac system," *Proc. - SPAWC 2023*, pp. 16–20, Nov 2023.
- [31] T. Lakkimsetti, U. M. Rao Ukyam, and K. Kumar Gurralla, "Power allocation for secure RIS-aided ISAC NOMA network," *Proc. - INDICON 2024*, pp. 1–6, Dec 2024.
- [32] F. Liu, C. Masouros, A. Li, H. Sun, and L. Hanzo, "Mu-mimo communications with mimo radar: From co-existence to joint transmission," *IEEE Trans. Wireless Commun.*, vol. 17, no. 4, pp. 2755–2770, Feb 2018.
- [33] X. Liu, T. Huang, N. Shlezinger, Y. Liu, J. Zhou, and Y. C. Eldar, "Joint transmit beamforming for multiuser MIMO communications and MIMO radar," *IEEE Trans. Signal Process.*, vol. 68, pp. 3929–3944, Jun 2020.
- [34] X. Liu, T. Huang, and Y. Liu, "Transmit design for joint mimo radar and multiuser communications with transmit covariance constraint," *IEEE J. Sel. Areas Commun.*, vol. 40, no. 6, pp. 1932–1950, Mar 2022.
- [35] L. Chen, Z. Wang, Y. Du, Y. Chen, and F. R. Yu, "Generalized transceiver beamforming for dfrc with mimo radar and mu-mimo communication," *IEEE J. Sel. Areas Commun.*, vol. 40, no. 6, pp. 1795–1808, Jun 2022.
- [36] Y. Ni, Z. Wang, and Q. Huang, "Joint transceiver beamforming for multi-target single-user joint radar and communication," *IEEE Wireless Commun. Lett.*, vol. 11, no. 11, pp. 2360–2364, Nov 2022.
- [37] J. Pritzker, J. Ward, and Y. C. Eldar, "Transmit precoder design approaches for dual-function radar-communication systems," *arXiv preprint arXiv:2203.09571*, 2022.
- [38] N. Zhao, Y. Wang, Z. Zhang, Q. Chang, and Y. Shen, "Joint transmit and receive beamforming design for integrated sensing and communication," *IEEE Commun. Lett.*, vol. 26, no. 3, pp. 662–666, Mar 2022.
- [39] Y. Li and M. Jiang, "Joint transmit beamforming and receive filters design for coordinated two-cell interfering dual-functional radar-communication networks," *IEEE Trans. Veh. Technol.*, vol. 71, no. 11, pp. 12362–12367, Jul 2022.
- [40] G. Interdonato, F. Di Murro, C. D'Andrea, G. Di Gennaro, and S. Buzzi, "Approaching massive mimo performance with reconfigurable intelligent surfaces: We do not need many antennas," *IEEE Trans. Commun.*, vol. 73, no. 6, pp. 4000–4016, Nov 2025.
- [41] B. He, F. Wang, and J. Cheng, "Joint secure transceiver design for integrated sensing and communication," *IEEE Trans. Wireless Commun.*, vol. 23, no. 10, pp. 13377–13393, Oct 2024.
- [42] Z. He, W. Xu, H. Shen, D. W. K. Ng, Y. C. Eldar, and X. You, "Full-duplex communication for isac: Joint beamforming and power optimization," *IEEE J. Sel. Areas Commun.*, vol. 41, no. 9, pp. 2920–2936, Jun 2023.
- [43] Z. Liu, S. Aditya, H. Li, and B. Clerckx, "Joint transmit and receive beamforming design in full-duplex integrated sensing and communications," *IEEE J. Sel. Areas Commun.*, vol. 41, no. 9, pp. 2907–2919, Sep 2023.
- [44] S. Bi, J. Lyu, Z. Ding, and R. Zhang, "Engineering radio maps for wireless resource management," *IEEE Wireless Commun.*, vol. 26, no. 2, pp. 133–141, Feb 2019.
- [45] Y. Cao, L. Duan, and R. Zhang, "Sensing for secure communication in isac: Protocol design and beamforming optimization," *IEEE Trans. Wireless Commun.*, vol. 24, no. 2, pp. 1207–1220, Feb 2025.
- [46] Y. Lu, K. Xiong, P. Fan, Z. Ding, Z. Zhong, and K. B. Letaief, "Secrecy energy efficiency in multi-antenna swipt networks with dual-layer ps receivers," *IEEE Trans. Wireless Commun.*, vol. 19, no. 6, pp. 4290–4306, Apr 2020.
- [47] W.-C. Li, T.-H. Chang, and C.-Y. Chi, "Multicell coordinated beamforming with rate outage constraint—part ii: Efficient approximation algorithms," *IEEE Trans. Signal Process.*, vol. 63, no. 11, pp. 2763–2778, Mar 2015.
- [48] Z. Sheng, H. D. Tuan, A. A. Nasir, T. Q. Duong, and H. V. Poor, "Power allocation for energy efficiency and secrecy of wireless interference networks," *IEEE Trans. Wireless Commun.*, vol. 17, no. 6, pp. 3737–3751, Jun 2018.
- [49] Z. Sheng, H. D. Tuan, T. Q. Duong, and H. V. Poor, "Beamforming optimization for physical layer security in miso wireless networks," *IEEE Trans. Signal Process.*, vol. 66, no. 14, pp. 3710–3723, May 2018.
- [50] K.-Y. Wang, T.-H. Chang, W.-K. Ma, A. M.-C. So, and C.-Y. Chi, "Probabilistic SINR constrained robust transmit beamforming: A bernstein-type inequality based conservative approach," *Proc. - ICASSP 2011*, pp. 3080–3083, May 2011.
- [51] J. Yang, B. Champagne, Q. Li, and L. Hanzo, "Secure MIMO AF relaying design: An intercept probability constrained approach," *Proc. - IEEE GLOBECOM*, pp. 1–6, Dec 2015.
- [52] Y. Zou, X. Wang, and W. Shen, "Intercept probability analysis of cooperative wireless networks with best relay selection in the presence of eavesdropping attack," *Proc. - IEEE ICC*, pp. 2183–2187, Jul 2013.
- [53] B. Li, J. Liao, X. Gong, H. Xiang, Z. Yang, and W. Zhao, "UAV-assisted ISAC network physical layer security based on stackelberg game," *Ad Hoc Netw.*, vol. 152, p. 103304, Jan 2024.
- [54] J. Sun, L. Yang, A.-A. A. Boulogeorgos, T. A. Tsiftsis, and H. Liu, "Dual-uav-aided covert communications for air-to-ground isac networks," *arXiv preprint arXiv:2506.00601*, 2025.
- [55] X. Wang, W. Feng, Y. Chen, and N. Ge, "Power allocation for UAV swarm-enabled secure networks using large-scale csi," *Proc. - IEEE GLOBECOM*, pp. 1–6, Dec 2019.
- [56] S. Lin, Y. Xu, H. Wang, and G. Ding, "Multi-antenna covert communication assisted by uav-ris with imperfect csi," *IEEE Trans. Wireless Commun.*, vol. 23, no. 10, pp. 13841–13855, Jun 2024.
- [57] Q. Wang, S. Guo, C. Wu, C. Xing, N. Zhao, D. Niyato, and G. K. Karagiannidis, "Star-ris aided covert communication in uav air-ground networks," *IEEE J. Sel. Areas Commun.*, vol. 43, no. 1, pp. 245–259, Sep 2025.
- [58] S. Li, H. Dong, C. Shan, X. Fang, W. Wu, and Z. Li, "Secure hybrid beamforming design for mmwave integrated sensing and communication systems," *IEEE Trans. Veh. Technol.*, pp. 1–16, Feb 2025.
- [59] J. An, H. Li, D. W. K. Ng, and C. Yuen, "Fundamental detection probability vs. achievable rate tradeoff in integrated sensing and communication systems," *IEEE Trans. Wireless Commun.*, vol. 22, no. 12, pp. 9835–9853, May 2023.
- [60] D. Xu, X. Yu, D. W. K. Ng, A. Schmeink, and R. Schober, "Robust and secure resource allocation for isac systems: A novel optimization framework for variable-length snapshots," *IEEE Trans. Commun.*, vol. 70, no. 12, pp. 8196–8214, Nov 2022.
- [61] R. Zhao, X. Hu, C. Liu, W. Wang, B. Liu, and K.-K. Wong, "Joint transmit and receive beamforming design for secure communications in isac systems with eavesdropper and jammer," *Proc. IEEE Chin. Int. Conf. Commun. (ICCC)*, pp. 885–890, Aug 2024.
- [62] Z. Liu, Z. Li, Y. Gong, and Y.-C. Wu, "RIS-aided cooperative mobile edge computing: Computation efficiency maximization via joint uplink and downlink resource allocation," *IEEE Trans. Wireless Commun.*, vol. 23, no. 9, pp. 11535–11550, Apr 2024.
- [63] L. Li, J. Zhang, and T.-H. Chang, "Beamforming optimization for robust sensing and communication in dynamic mmwave mimo networks," *IEEE J. Sel. Areas Commun.*, vol. 43, no. 4, pp. 1354–1370, Jan 2025.
- [64] S. Lu, I. Tsaknakis, M. Hong, and Y. Chen, "Hybrid block successive approximation for one-sided non-convex min-max problems: Algorithms and applications," *IEEE Trans. Signal Process.*, vol. 68, pp. 3676–3691, Apr 2020.
- [65] A. Beck, *First-Order Methods in Optimization*. Philadelphia, PA: Society for Industrial and Applied Mathematics, 2017.
- [66] B. Zhou, L. Gao, and Y.-H. Dai, "Gradient methods with adaptive step-sizes," *Comput. Optim. Appl.*, vol. 35, pp. 69–86, Mar 2006.
- [67] J. Zhang, P. Xiao, R. Sun, and Z. Luo, "A single-loop smoothed gradient descent-ascent algorithm for nonconvex-concave min-max problems," *Proc. - Adv. Neural Inf. Process. Syst. (NeurIPS)*, vol. 33, pp. 7377–7389, 2020.

- [68] J. He, H. Zhang, and Z. Xu, "An approximation proximal gradient algorithm for nonconvex-linear minimax problems with nonconvex nonsmooth terms," *J. Glob. Optim.*, vol. 90, no. 1, pp. 73–92, Mar 2024.
- [69] Z. Xu, H. Zhang, Y. Xu, and G. Lan, "A unified single-loop alternating gradient projection algorithm for nonconvex-concave and convex-nonconcave minimax problems," *Math. Program.*, vol. 201, no. 1, pp. 635–706, Jan 2023.
- [70] M. Nouiehed, M. Sanjabi, T. Huang, J. D. Lee, and M. Razaviyayn, "Solving a class of non-convex min-max games using iterative first order methods," *Proc. Adv. Neural Inf. Process. Syst. (NeurIPS)*, vol. 32, 2019.
- [71] W. Yuanhao, Z. Guodong, and B. Jimmy, "On solving minimax optimization locally: A follow-the-ridge approach." *Proc. - Int. Conf. Learn. Represent. (ICLR)*, Apr 2020.
- [72] S. Lu, K. Zhang, T. Chen, T. Başar, and L. Horesh, "Decentralized policy gradient descent ascent for safe multi-agent reinforcement learning," *Proc. - AAAI Conf. Artif. Intell.*, vol. 35, no. 10, pp. 8767–8775, 2021.
- [73] T. Lin, C. Jin, and M. I. Jordan, "Near-optimal algorithms for minimax optimization," *Proc. - Conf. Learn. Theory.*, pp. 2738–2779, 2020.
- [74] H. T. Davis, *The summation of series*. Courier Dover Publications, 2014.
- [75] Z. Li, M. Xia, M. Wen, and Y.-C. Wu, "Massive access in secure noma under imperfect csi: Security guaranteed sum-rate maximization with first-order algorithm," *IEEE J. Sel. Areas Commun.*, vol. 39, no. 4, pp. 998–1014, Aug 2021.
- [76] S. Xu, Y. Cheng, S. Wang, X. Wang, Z. Zheng, and Z. Fei, "Mutual information-oriented isac beamforming design for large dimensional antenna array," *Electronics*, vol. 14, no. 13, p. 2515, Jun 2025.
- [77] S. He, K. Tang, B. Zheng, X. Xiu, W. Feng, W. Che, and Q. Xue, "Throughput maximization design for RIS-assisted WPCN-NOMA-based ISAC systems," *IEEE Trans. Commun.*, vol. 73, no. 8, pp. 6943 – 6957, Feb 2025.
- [78] D. Tse and P. Viswanath, *Fundamentals of Wireless Communication*. Cambridge University Press, 2005.
- [79] Z. Liu, L. Yin, W. Shin, and B. Clerckx, "Rate-splitting multiple access for quantized isac leo satellite systems: A max-min fair energy-efficient beam design," *IEEE Trans. Wireless Commun.*, vol. 23, no. 10, pp. 15 394–15 408, Jul 2024.